DOI: 10.1002/ejic.200800859

Lanthanide(III) Complexes of Phosphorus Acid Analogues of H_4DOTA as Model Compounds for the Evaluation of the Second-Sphere Hydration

Zuzana Kotková,[a] Giovannia A. Pereira,[b] Kristina Djanashvili,[c] Jan Kotek,[a] Jakub Rudovský,[a] Petr Hermann,[a] Luce Vander Elst,[d] Robert N. Muller,[d] Carlos F. G. C. Geraldes,[b] Ivan Lukeš,*[a] and Joop A. Peters*[c]

Keywords: Contrast agents / Lanthanides / NMR spectroscopy / Phosphinate complexes / Phosphonate complexes

Five DOTA-like ligands lacking a water molecule in the first coordination sphere of their Gd^{III} complexes, namely the phosphinates H_4DOTP^{H}, H_4DOTP^{hm} and H_4DOTP^{Et}, and the phosphonate monoesters H_4DOTP^{OEt} and H_4DOTP^{OBu}, were synthesized with the aim of exploring the influence of the second hydration sphere on the relaxivity of Gd^{III} complexes. The H_4DOTP^{H}, H_4DOTP^{hm} and H_4DOTP^{OEt} ligands and their Ln^{III} complexes were characterized by potentiometry and time-resolved luminescence; the Gd^{III} complexes are thermodynamically much less stable than that of H_4DOTA, and no water is coordinated in the inner sphere. The crystal structures of the free ligand H_4DOTP^{OEt} and of the Gd^{III} complexes of H_4DOTP^{H} and H_4DOTP^{OEt} were determined by X-ray diffraction. The complexes have the expected octadentate coordination mode with an N_4O_4 arrangement; no water molecule is bound to the Gd^{III} ion. Information on the structures of the Ln^{III} complexes of all five ligands in aqueous solution were obtained from ^{1}H and ^{31}P NMR spectra. The NMR spectra of the $[Ln(DOTP^{hm})]^-$ and $[Ln(DOTP^{Et})]^-$ complexes show that these compounds have a clear preference for a specific arrangement of phosphorus atoms which gives rise to the symmetrical *RRRR* (or *SSSS*) isomer. However, many diastereoisomers were observed for all other complexes. Ln^{III}-induced ^{17}O NMR shift data reveal that the spatial location of the second-sphere water molecules for the two groups of complexes differs. The parameters governing the effect of the second hydration sphere on the relaxivity of the Gd^{III} complexes of all ligands were evaluated by EPR, variable-temperature ^{17}O NMR spectroscopy and ^{1}H NMRD relaxometry. The presence of second-sphere water molecules is clearly confirmed, depending on the character of the pendant arms. As the relaxivity does not depend significantly on the nature of the phosphorus substituents and/or on the isomerism present in solution, the second-sphere water molecules should be located close to the phosphorus–oxygen atoms.

Introduction

Magnetic resonance imaging (MRI) is one of the most widely used medical diagnostic techniques. Gadolinium(III)-based contrast agents (CAs) have significantly extended the applicability of this imaging method, and optimizing the efficacy of CAs has been an important goal for more than a decade.[1–5] The research undertaken has led to a much better understanding of the parameters governing the effectiveness of these CAs, which is usually expressed by the relaxivity (the enhancement of the water proton relaxation rate in a 1 mM solution of CA).[1–6] The structure of the ligand can be tuned to optimize some of the parameters for optimal contrast efficiency, including the rotational correlation time (τ_R), the number of water molecules directly bound to the central metal ion (q) and their residence time in the first coordination sphere (τ_M). These parameters mainly influence the so-called inner-sphere contribution to the overall relaxivity. Other parameters, such as the electronic relaxation rates ($T_{1e,2e}$) of the Gd^{III} ion[1,2,7,8] or the contribution of water molecule(s) in the second hydration sphere,[9] are less well understood.

The second-sphere contribution to the relaxivity originates from water molecules held in the close proximity to the Gd^{III} ion by hydrogen bonds to the organic ligand of the complex.[9] This contribution can enhance the overall relaxivity by 5–15% depending on the structure of the complex. Some years ago, it was demonstrated that complexes

[a] Department of Inorganic Chemistry, Univerzita Karlova (Charles University),
Hlavova 2030, 12840 Prague, Czech Republic
Fax: +420-22195-1253
E-mail: lukes@natur.cuni.cz
[b] Departamento de Bioquímica, Faculdade de Ciências e Tecnologica, e Centro de Neurociências, Universidade de Coimbra, 3049 Coimbra, Portugal
[c] Laboratory for Biocatalysis and Organic Chemistry, Department of Biotechnology, Delft University of Technology, Julianalaan 136, 2628 BL Delft, The Netherlands
Fax: +31-152-784-289
E-mail: j.a.peters@tudelft.nl
[d] NMR Laboratory, Department of Organic Chemistry, University of Mons-Hainaut, 7000 Mons, Belgium

Supporting information for this article is available on the WWW under http://www.eurjic.org or from the author.

of phosphorus-containing ligands exhibit a higher hydration (i.e. more extended second hydration sphere) than complexes of carboxylate ligands. This is particularly true for lanthanide(III) complexes of H_8DOTP [H_8DOTP = 1,4,7,10-tetraazacyclododecane-1,4,7,10-tetrakis(methylphosphonic acid), Scheme 1], whose Gd^{III} complex does not contain any directly coordinated water molecule[10] but has a relaxivity (r_1) comparable to that of the clinically used $[Gd(H_2O)(DOTA)]^-$ complex (H_4DOTA = 1,4,7,10-tetraazacyclododecane-1,4,7,10-tetraacetic acid, Scheme 1), which has one water molecule in the first coordination sphere.[11] The water relaxation enhancement by the DOTP complex results exclusively from the second-sphere contribution after conjugation to a macromolecule.[12] A previous relaxometric study concerning Gd^{III} complexes of the related ethylphosphinate ligand (H_4DOTP^{Et}), and of the ethyl- and butylphosphonate monoesters (H_4DOTP^{OEt} and H_4DOTP^{OBu}, respectively), indicated only poor hydration (coordination number lower than one).[13] The absence of directly coordinated water molecules and the presence of second-sphere water molecule(s) has been demonstrated for Gd^{III} complexes of phosphinic acid analogues of H_4DOTA having methyl (H_4DOTP^{Me}),[14] phenyl (H_4DOTP^{Ph})[15] or benzyl (H_4DOTP^{Bn})[16] substituents on the phosphorus atom (Scheme 1).

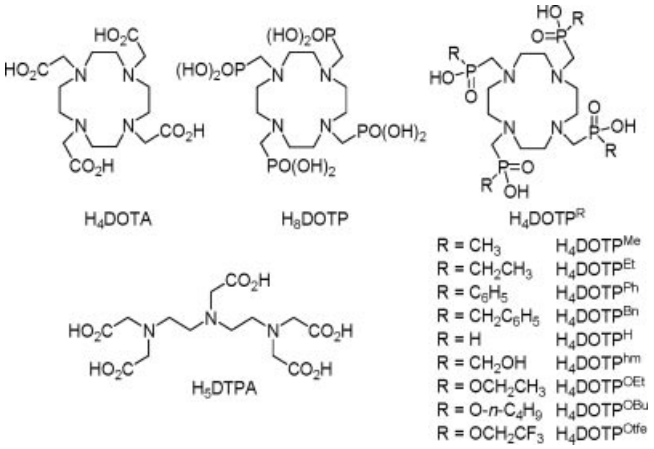

Scheme 1. Formulas of ligands mentioned in the text.

The structures of complexes of these tetraphosphorus acid derivatives are analogous to those of complexes of the parent ligand H_4DOTA, where the lanthanide(III) ion is sandwiched between N_4- and O_4-planes. The H_4DOTA complexes are present in solution in two diastereoisomeric forms that differ in the mutual rotation of N_4- and O_4-planes to give a square-antiprismatic (SA) arrangement [torsion angle >35°, with opposite signs of rotation of the pendant arms (Δ/Λ) and the conformation of the ethylene bridges in the macrocycle ring (δ/λ), represented as the Δ-λλλλ/Λ-δδδδ isomeric pair, traditionally termed "**M**"] and a twisted-square-antiprismatic (TSA) arrangement (torsion angle <30°, with the same sign of rotation leading to Λ-λλλλ/Δ-δδδδ antipodes, traditionally termed "**m**").[17] Complexes of H_4DOTP^R ligands, on the other hand, occur exclusively in a TSA arrangement as their pendant arms contain more bulky phosphorus atoms.[10,15,16,18,19] The presence of just one phosphorus-based pendant arm causes an increased population of the TSA isomer.[20–24] As stated above, the Gd^{III} complexes of all the tetraphosphorus ligands under study have no coordinated water molecules. In fact, direct coordination of a water molecule was observed, in the solid state, only for the La^{III} and Ce^{III} complexes.[15,16b]

A rich, second-sphere hydration has also been observed in Gd^{III} complexes of pyridine-containing macrocycles containing phosphonic acid pendant arms.[25] It has been shown recently that the second-sphere contribution to the overall relaxivity is significant even in complexes of H_5DTPA (H_5DTPA = 1,4,7-triazaheptane-1,1,4,7,7-pentaacetic acid, Scheme 1)[26] or H_4DOTA derivatives containing only one phosphonic/phosphinic acid group.[20–22] This contribution was found to be more pronounced when complexes of these monophosphorus acid ligands were bound to macromolecules.[27,28] Theoretical approaches to treat the second-sphere hydration have confirmed that phosphonic acid groups enhance the hydration of complexes of DOTA-like ligands[29] as well as of open-chain ligands.[30] In this paper, we evaluate the second-sphere contribution to the overall relaxivity in a series of Ln^{III} complexes of tetraphosphorus acid analogues of H_4DOTA with phosphinic (H_4DOTP^H), hydroxymethylphosphinic (H_4DOTP^{hm}), ethylphosphinic (H_4DOTP^{Et}) and phosphonate ethyl monoester (H_4DOTP^{OEt}) and butyl monoester (H_4DOTP^{OBu}) pendant arms (Scheme 1) by means of a combination of relaxometric and other spectroscopic methods. In addition, the influence of the substituent on the phosphorus atom to this contribution is investigated.

Results and Discussion

Syntheses

H_4DOTP^H was prepared by a Mannich reaction between cyclen, paraformaldehyde and hypophosphorous acid according to a slightly modified literature procedure;[31] milder conditions were applied, for this reaction and during the workup, to reduce the amount of by-products, including derivatives with various numbers of pendant arms with hydroxymethyl and hydrogen substituents (e.g. intermediates in H_4DOTP^{hm} formation) and partially *N*-methylated derivatives of cyclen having a smaller number of phosphinate pendants. Despite the optimized reaction conditions, the amount of by-products was still high, and the yield of isolated product was only 20%. H_4DOTP^{hm} was obtained as a by-product during the synthesis of H_4DOTP^H, but could also be prepared more conveniently from pure H_4DOTP^H upon treatment with an excess of paraformaldehyde. In this way, less by-products were present in the final reaction mixture and the isolated yield of H_4DOTP^{hm} was 50%. H_4DOTP^{OEt} was prepared by treating cyclen with paraformaldehyde and triethyl phosphite (without solvent) at 40 °C.[32] The octaethyl ester Et_8DOTP obtained was hydrolyzed in aqueous NaOH to give the desired product in

an overall yield of 90%. H_4DOTP^{Et} and H_4DOTP^{OBu} were synthesized according to literature procedures.[13,33] All ligands were purified, as mentioned in the Experimental Section, to a purity of at least 99%. The lanthanide(III) complexes were formed at a pH around 7 and at room temperature in 1 h (confirmed by ^{31}P NMR spectroscopy), which demonstrates that the complexation rates are rapid.

Crystal Structures

Crystal Structure of $H_4DOTP^{OEt}\cdot H_2O$

The structurally independent unit in the crystal structure of $H_4DOTP^{OEt}\cdot H_2O$ contains two ligand molecules, with similar conformations, and two solvate water molecules (see Figure 1 and Figure S1 in the Supporting Information). The free ligand H_4DOTP^{OEt} crystallizes as a zwitterion, with two (mutually "*trans*") macrocycle nitrogen atoms protonated. The two remaining protons are bound to the pendant phosphonate groups attached to the unprotonated amino groups in opposite positions. The macrocyclic part adopts a conformation typical for doubly protonated substituted cyclens, with intramolecular hydrogen bonds between protonated and unprotonated amino groups and all substituents pointing in the same direction with respect to the macrocyclic plane.[34] Both protonated pendant arms are turned above the macrocycle (and participate in hydrogen bonding with protonated amino groups), and the remaining two pendants are turned outwards from the macrocycle cavity. The quality of the crystal data was rather poor – some ethyl ester groups and the solvate water molecules were found to be disordered. A similar orientation of the pendant arms is also found in the structures of the parent H_8DOTP[35] and H_4DOTA.[36]

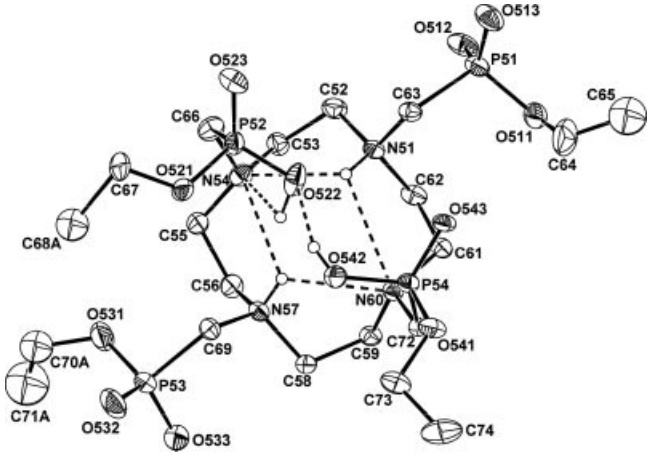

Figure 1. Molecular structure of one independent ligand molecule found in the crystal structure of $H_4DOTP^{OEt}\cdot H_2O$, showing the intramolecular hydrogen bonds (dashed). Hydrogen atoms attached to carbon atoms have been omitted for clarity. Only one position of the disordered parts of molecule (phosphonate ester groups) is shown.

Crystal Structure of $Li[Gd(DOTP^H)]\cdot 6H_2O$

The central Gd^{III} ion in the crystal structure of $Li[Gd(DOTP^H)]\cdot 6H_2O$ (Figure 2) is coordinated to four nitrogen atoms of the macrocycle and four oxygen atoms of the pendant arms to form two parallel N_4- and O_4-planes. As the complex possesses the symmetry of a crystallographic twofold axis, only half of the molecule forms the independent unit. The sign of rotation of the pendant arms (Λ/Δ) is the same as that of the conformation of the ethylene bridges in the macrocycle ring (δ/λ). This leads to a TSA (Λ-λλλλ/Δ-δδδδ) environment and confirms the results found by NMR spectroscopy (see below). The torsion angle between the N_4- and O_4-planes is about 30°, which is typical for a TSA coordination sphere [an SA isomer (Δ-λλλλ/Λ-δδδδ) would typically have a torsion angle of more than 35°].[23,24] The O22 oxygen atom of one pendant arm was best fitted as disordered in two positions with relative occupancies 60(A):40(B), with the phosphinate hydrogen atom placed in the theoretical position. This leads to two diastereoisomers (each of which is present in both enantiomeric forms as the space group is centrosymmetric), namely *SSSS*-Δ-δδδδ (+*RRRR*-Λ-λλλλ) and *SRSR*-Δ-δδδδ (+*SRSR*-Λ-λλλλ). The opening angles O–Gd–O are around 125°, which is too small for the coordination of a water molecule.[37]

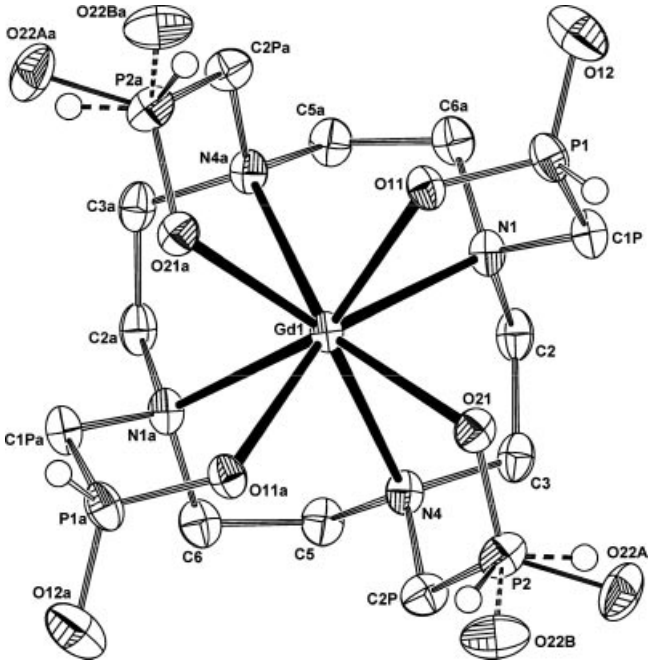

Figure 2. Molecular structure of the $[Gd(DOTP^H)]^-$ species found in the crystal structure of $Li[Gd(DOTP^H)]\cdot 6H_2O$. Hydrogen atoms attached to carbon atoms have been omitted for clarity. Both positions of the disordered phosphinate pendant arm, with *SSSS*-Δ-δδδδ (60%, O22A) and *SRSR*-Δ-δδδδ (40%, O22B) configurations, are shown.

The molecules in this complex are packed in a polymeric chain due to coordination through the lithium counterion. This ion was also refined as being disordered over two positions as it is coordinated by the disordered oxygen atom O22. The coordination sphere of the lithium ion is completed by two water molecules, which are located far from the metal centre and the pseudo-C_4 axis (the closest Gd···Ow distance is 5.67 Å and the QN–QO–Ow angle is

Table 1. Selected geometrical parameters found in the crystal structures of Li[Gd(DOTP^{H})]·6H_2O and Li[Gd(DOTP^{OEt})]·0.5Me_2CO·8H_2O.

	Li[Gd(DOTP^{H})]·6H_2O	Li[Gd(DOTP^{OEt})]·0.5Me_2CO·8H_2O	
		Molecule 1	Molecule 2
Distances [Å]			
Gd1–N1	2.636(2)	2.663(4)	2.693(5)
Gd1–N4	2.635(2)	2.667(4)	2.670(5)
Gd1–N7	–	2.662(5)	2.649(5)
Gd1–N10	–	2.665(4)	2.670(5)
Gd1–O11	2.311(2)	2.315(4)	2.320(3)
Gd1–O21	2.319(2)	2.332(4)	2.308(3)
Gd1–O31	–	2.323(4)	2.315(3)
Gd1–O41	–	2.307(4)	2.307(4)
Gd1–QN [a]	1.6053(2)	1.6390(2)	1.6520(2)
Gd1–QO [a]	1.0503(2)	1.0495(2)	1.0491(2)
Angles [°]			
O11–Gd1–O31	124.6(1)[b]	124.7(1)	127.2(1)
O21–Gd1–O41	127.4(1)[b]	127.6(1)	124.9(1)
N1–QN–QO–O11[a]	29.21(8)	26.7(2)	27.7(2)
N4–QN–QO–O11[a]	30.50(8)	27.4(2)	26.1(2)
N7–QN–QO–O11[a]	–	27.0(2)	28.2(2)
N10–QN–QO–O11[a]	–	28.6(2)	26.3(2)
N_4-plane–O_4-plane	0	1.09(2)	0.86(3)

[a] QN is the centroid (centre of gravity) of the N_4-plane and QO the centroid of the O_4-plane. [b] O31/O11$^{\#}$ and O41/O21$^{\#}$ are related by a twofold symmetry axis; $^{\#}$: $-x$, y, $-z$ + 1/2.

around 98°, where QN is the centroid of the N_4-plane and QO the centroid of the O_4-plane). Selected geometrical parameters are listed in Table 1.

Crystal Structure of Li[Gd(DOTP^{OEt})]·0.5Me_2CO·8H_2O

The independent part of the crystal structure of Li[Gd(DOTP^{OEt})]·0.5Me_2CO·8H_2O (Figure 3) consists of two complex molecules. Similarly to the previous case, the central Gd^{III} ions in both molecules are coordinated by four nitrogen atoms of the macrocycle and four oxygen atoms of the pendant arms to form two parallel N_4- and O_4-planes. The stereochemistry of the complex molecules is also TSA (Λ-λλλλ/Δ-δδδδ), with torsion angles between the N_4- and O_4-planes of about 28°. The absolute configuration of the phosphonate monoesters is alternating, leading to *SRSR*-Δ-δδδδ and *SRSR*-Λ-λλλλ species, as was observed in the case of H_4DOTP^{Ph} complexes.[15] One of the lithium counterions is coordinated by O23X and by three water molecules in an approximately tetrahedral arrangement. The other lithium ion is tetrahedrally coordinated by four water molecules. Similarly to the previous structure, the water molecules are located away from the metal centre and the pseudo-C_4 axis of the complexes (the distances of the closest water molecules from metal centre are in the range 5.37–5.60 Å, with corresponding QN–QO–Ow angles of 97–102°). Selected geometrical parameters are listed in Table 1.

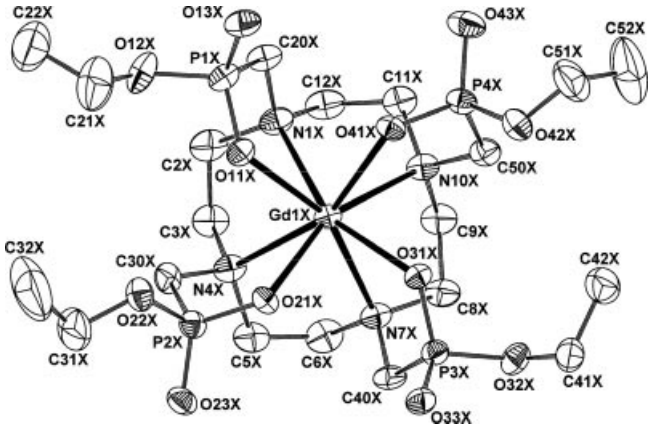

Figure 3. Molecular structure of one (the independent molecule labelled X) of the [Gd(DOTP^{OEt})]$^-$ species found in the crystal structure of Li[Gd(DOTP^{OEt})]·0.5Me_2CO·8H_2O. Hydrogen atoms have been omitted for the sake of clarity. The picture shows the species with *SRSR*-Δ-δδδδ configuration.

Potentiometry

Protonation Constants of the Ligands

The protonation constants of the free ligands are given in Table 2. These ligands adopt the general protonation scheme of DOTA-like compounds. The first two protonations occur on macrocyclic nitrogen atoms (with pK_a values of about 10–11 and 7–8, respectively). The overall basicity of the macrocyclic nitrogen atoms [pK(HL) + pK(H_2L) = logβ(H_2L)] is rather low and corresponds well to the generally observed order phosphinates ≈ phosphonate monoesters < carboxylates < phosphonates (Table 2).[37] The proton dissociation constants of the H_2L^{2-} species of the ligands studied, as well as those of H_4DOTP^{Ph} (ref.[38]) and H_4DOTP^{Otfe} (ref.[39]), depend on the electronic properties of the substituent on the phosphorus atoms, in agreement with previous observations on simple aminomethylphosphinic acids – more electronegative substituents result in lower pK_a values.[40] The protonations in the acidic region

Table 2. Protonation constants[a] and corresponding pK_a values[b] of the studied ligands.

h	Species[c]	H_4DOTP^{H}[d]		H_4DOTP^{hm}[d]		H_4DOTP^{Et}[e]	H_4DOTP^{OEt}[f]	H_4DOTP^{OBu}[g]	H_8DOTP[h]	H_4DOTA[i]
		$\log\beta_h$	pK_a	$\log\beta_h$	pK_a	pK_a	pK_a	pK_a	pK_a	pK_a
1	HL	10.58(2)	10.58	10.60(2)	10.60	10.94	11.57	10.34	>13	11.9
2	H_2L	17.51(3)	6.93	18.46(2)	7.86	8.24	7.94	7.72	12.45	9.72
3	H_3L	19.41(3)	1.90	20.21(3)	1.75	3.71	1.80	2.42	9.18	4.60
4	H_4L	–	–	21.13(5)	0.92	–	–	–	7.95	4.13
5	H_5L	–	–	–	–	–	2.3 [j]	–	6.08	2.36
6	H_6L	–	–	–	–	–	–	–	5.20	–
7	H_7L	–	–	–	–	–	–	–	1.85	–

[a] $\beta_h = [H_hL^{(h-4)}]/([H^+]^h \times [L^{4-}])$. [b] p$K_a = \beta_h - \beta_{h-1}$. [c] Charges have been omitted for clarity. [d] This work. [e] Ref.[41] [f] Ref.[32] [g] Ref.[33] [h] Ref.[42] [i] Ref.[43] [j] Simultaneous deprotonations over two steps.

(pK_a < 2–3) can be assigned to those of the phosphinate/phosphonate monoester moieties and/or the remaining macrocyclic amino groups.

Stability of the Gadolinium(III) Complexes

The stability constants of complexes with phosphinate and phosphonate monoester ligands (Table 3) are much lower than those of the parent ligands H_8DOTP and H_4DOTA, which can be ascribed to the lower overall basicity of the ligands. Consequently, the complexes are formed at higher pH – the Gd^{III} ion, for example, is only fully complexed above a pH of about 5. The distribution diagram for Gd^{III}-containing species in the Gd^{III}-H_4DOTP^{OEt} system under equilibrium conditions is shown in Figure 4 as an example. The proton dissociation constants of the

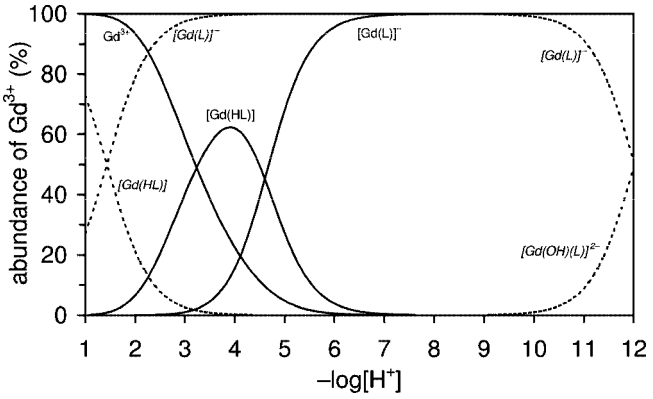

Figure 4. Distribution of Gd^{III}-containing species in the Gd^{III}/H_4DOTP^{OEt} ($H_4DOTP^{OEt} = H_4L$) system under equilibrium conditions [$c(Gd^{III}) = c(H_4L) = 0.004$ M; full lines]. Distribution of Gd^{III}-containing species during titration of the pre-formed $[Gd(L)]^-$ complex ($c\{[Gd(L)]^-\} = 0.004$ M; dashed lines, formulae in italics). The protonated [Gd(HL)] species probably bind the proton at a nitrogen atom under equilibrium conditions and an oxygen atom in the pre-formed complex.

$[Gd(HDOTP^{R,OR})]$ species (formally the [*hlm*] = [111] species) are relatively high at around 4. This suggests that the proton in these species is probably bound to a nitrogen atom in the macrocycle under the equilibrium conditions, in other words the macrocycle is not fully coordinated, and the Gd^{III} ion is bound mainly by the oxygen atoms of the pendant arms. Proton removal from the protonated species leads to full coordination of the ligand in the normal N_4O_4 mode. The potentials do not change after prolonged standing of the samples – the same values were observed after six weeks as after three weeks, which confirms that thermodynamic equilibrium was reached in the solutions used. Although these Ln^{III} complexes have a relatively low thermodynamic stability, they have a high kinetic stability both in vitro and in vivo.[32]

Protonation of the Gadolinium(III) Complexes

The relaxivity of $[Gd(DOTP^{hm})]^-$ appears to be dependent on the pH (see below), whereas the relaxivity of the other complexes is pH-independent. To gain more insight into the observed behaviour, we performed a potentiometric study of pre-formed Gd^{III} complexes of H_4DOTP^{hm} and, for comparison, of H_4DOTP^{OEt}. During these measurements, we explored the kinetically controlled pseudo-equilibrium associated with the complex protonation as the complexes are kinetically stable under these conditions. Solutions of the Gd^{III} complexes of H_4DOTP^{hm} and H_4DOTP^{OEt} were prepared in sealed ampoules (see Experimental Section) and used for the determination of their protonation/dissociation constants. The obtained constants are given in Table 4, and the corresponding distribution diagram is shown in Figure 4. The $[Gd(HDOTP^{R,OR})]$ complexes behave as monovalent strong acids with a pK_a of about 1.4. Such dissociation constants correspond well with those of the pendant arms in the free ligands, although the pK_a values are somewhat lower in the complexes due to the

Table 3. Stability constants[a] of gadolinium(III) complexes of the studied ligands.

h	l	m	H_4DOTP^{H}[b]	H_4DOTP^{hm}[b]	H_4DOTP^{Et}[c]	H_4DOTP^{OEt}[b]	H_4DOTP^{OBu}[d]	H_8DOTP[e]	H_4DOTA[f]
			$\log\beta_{hlm}$	$\log\beta_{hlm}$	$\log\beta_{hlm}$	$\log\beta_{hlm}$	$\log\beta_{hlm}$	$\log\beta_{hlm}$	$\log\beta_{hlm}$
0	1	1	14.0(1)	16.09(4)	16.50	14.4(2)	12.19	28.8	24.67
1	1	1	18.11(5)[g]	19.25(5)[g]	–	19.0(1)[g]	–	36.4[g]	–
			4.1	*3.2*		*4.6*		*7.6*	

[a] $\beta_{hlm} = [H_hL_lM_m^{h-4l+3m}]/([H^+]^h \times [L^{4-}]^l \times [M^{3+}]^m)$. [b] This work. [c] Ref.[41] [d] Ref.[33] [e] Ref.[44]; the other pK_a values are: 6.3, 5.4 and 4.0. [f] Ref.[45] [g] The corresponding pK_a values are given in italics.

coordination of the pendant arms. Thus, the low pK_a value points to the kinetic inertness of the complex species, at least on the time scale of the potentiometric measurements, and that the complexes are protonated at an oxygen atom of the pendant arms. As no other protonations occur in the pH range 3–10, the relaxivity change observed for the $[Gd(DOTP^{hm})]^{-}$ complex in this region (see below) cannot be associated with the presence of any protonation/deprotonation event (e.g. dissociation of a proton from the PCH_2OH groups); therefore, the relaxivity change must be associated with the H^+/OH^- catalysis of the prototropic exchange.[36,46]

Table 4. Equilibrium constants (pK_a) of the pre-formed Gd^{III} complexes with H_4DOTP^{hm} and H_4DOTP^{OEt}.

Equilibrium	$[Gd(DOTP^{hm})]^-$	$[Gd(DOTP^{OEt})]^-$
$[HML] \rightleftharpoons H^+ + [ML]^-$	1.39(3)	1.43(3)
$[ML]^- \rightleftharpoons H^+ + [H_{-1}ML]^{2-}$	11.29(1)	12.01(2)

Interestingly, the fits of the potentiometric data improved dramatically after inclusion of deprotonated species (pK_a of around 12) in the chemical model. Since deprotonated species were observed for the complexes of both H_4DOTP^{hm} and H_4DOTP^{OEt}, this improvement cannot be explained by dissociation of a hydroxymethyl moiety of the former complex. As no water is coordinated in the inner sphere of the complexes (see below), the deprotonation can only be explained by coordination of a hydroxide anion after decoordination of one of the pendant arms. Such behaviour points to a relatively weak coordination of the phosphinic acid or phosphonic monoester functions, probably due to the low nucleophilicity of their oxygen atoms[37] and the high affinity of lanthanide(III) ions for the hydroxide anion.

From the distribution diagram (Figure 4) and published data on other lanthanide(III) complexes,[32] it is clear that the pre-formed $[Gd(DOTP^{R,OR})]^-$ complexes are kinetically relatively inert on the potentiometry time scale (ca. 20 min). Above a pH of about 4, the concentration of the $[Gd(HDOTP^{R,OR})]$ species is negligible. Since the most likely mechanism of dissociation of the complex involves protonation of the pendant arm followed by proton transfer to the nitrogen atoms and subsequent dissociation of the complex, it may be concluded that the complexes are stable under the experimental conditions applied for the investigation of the pH dependence of the ^1H NMRD profiles (see below).

Luminescence and UV/Vis Measurements of Eu^{III} Complexes

To confirm the absence of a directly coordinated water molecule in the Gd^{III} complexes studied, we measured luminescence lifetimes of the excited states of selected Eu^{III} complexes in H_2O and D_2O (see Table S1 in the Supporting Information).

The luminescence lifetimes obtained for the $[Eu(DOTP^{OEt})]^-$ and $[Eu(H_{1.5}DOTP)]^{3.5-}$ (pH ≈ 7) complexes in H_2O solution are relatively long compared to those for complexes with one coordinated water molecule {e.g. $[Eu(H_2O)(DOTA)]^-$, where the lifetimes observed in H_2O are about 650 μs}, but still significantly shorter than the lifetimes measured in D_2O solution. For $[Eu(DOTP^H)]^-$ and $[Eu(DOTP^{hm})]^-$ complexes, the lifetimes observed in H_2O are even closer to the values of $[Eu(H_2O)(DOTA)]^-$ itself. However, using the relevant equations published in the literature,[47,48] the hydration number, q, was estimated to be 0.3–0.7 (Table S1 in the Supporting Information). This fact is usually attributed to a partial hydration of the complexes (i.e. equilibrium between complex species with $q = 0$ and 1, respectively). Alternatively, a high second-sphere hydration also gives such an effect.[48] As the published equations used to calculate q were derived mostly for amide derivatives, which have a lower second-sphere hydration, the correction for second-sphere contribution can be underestimated. In our case, the richer hydration sphere of the phosphorus acid complexes contributes more to the decay rates. All in all, however, the luminescence data do not allow an unambiguous conclusion regarding the value of q for the Eu^{III} complexes of the tetraphosphorus acid derivatives; therefore, we recorded absorption spectra for the $^5D_0 \leftarrow {}^7F_0$ transition. Only a single symmetrical absorption peak was observed in the spectra (Figure S2 in the Supporting Information). Since the $^5D_0 \leftarrow {}^7F_0$ transition is extremely sensitive to the local coordination environment of the central Eu^{III} ion, a change in hydration [i.e. change in coordination number (CN) between 8 and 9] would have resulted in a substantial difference in the corresponding two spectral bands with a separation of the peaks typically larger than 0.5 nm.[30,49] We can therefore conclude that only non-hydrated complex species (i.e. having CN = 8) are present in the solutions; the luminescence lifetimes given above (i.e. slight shortening of τ_{H_2O} in comparison with τ_{D_2O}) should be significantly shorter for any hydrated complex. The non-zero hydration numbers (q = 0.4–0.6) calculated from the luminescence lifetimes are therefore due to the effect of the second-sphere water molecules and/or of neighbouring OH oscillators in the case of the $[Eu(DOTP^{hm})]^-$ complex.[48]

NMR Studies of the Complexes

^{31}P and ^1H NMR Spectra

^1H and ^{31}P NMR spectra of the complexes with Nd^{III}, Eu^{III} and Yb^{III} were recorded in order to obtain information about the solution structure of the complexes. It is well known that all lanthanide(III) complexes of tetraphosphonate/phosphinate analogues of H_4DOTA selectively adopt TSA-type (Λ-λλλλ/Δ-δδδδ) structures.[10,15,16,18,19] However, since the presently studied ligands have a substituent on the phosphorus atoms, four additional chirality centres are created upon coordination of the prochiral phosphorus atoms, which leads to *R*/*S* isomerism centred on the phosphorus atoms. Six diastereoisomers (*RRRR*, *RRRS*, *RRSS*, *RSRS*, *SSSR* and *SSSS*) with a relative statistical abundance of 1:4:4:2:4:1 are therefore possible for the TSA arrangement. This, in principle, gives rise to a

quite complicated isomeric mixture. The isomerism of the lanthanide(III) complexes with analogous ligands such as $DOTP^{Otfe}$ (ref.[39]) and $DOTP^{Ph}$ (ref.[15]) has been discussed in detail previously.

The ^{31}P NMR spectra of the $[Eu(DOTP^{H})]^-$, $[Eu(DOTP^{OEt})]^-$ and $[Eu(DOTP^{OBu})]^-$ complexes show the full set of possible isomers (sixteen ^{31}P NMR signals for the six isomers) with no predominant isomer, as observed previously for other complexes.[15,39] The ^{31}P NMR spectra of the Yb^{III} and Nd^{III} complexes of H_4DOTP^{H}, H_4DOTP^{OEt}, and $DOTP^{OBu}$ show a similar pattern (Figures S3, S6 and S7 in the Supporting Information). The ^{31}P NMR spectra of the $[Eu(DOTP^{hm})]^-$ and $[Eu(DOTP^{Et})]^-$ complexes, on the other hand, are quite simple, with one major signal (integral intensity ca. 70%) and four minor ones (integral ratio 1:1:1:1, total integral intensity ca. 25%) being present in the spectra of the $[Eu(DOTP^{hm})]^-$ complex (Figure S4 in the Supporting Information). The major resonance can be assigned to the totally symmetric *RRRR* (or *SSSS*) and the four minor resonances to the *RRRS* (or *SSSR*) isomers, respectively. Signals for other possible diastereomers are negligible (total integral intensity <5%). The Yb^{III} and Nd^{III} complexes of H_4DOTP^{hm} and H_4DOTP^{Et} also have ^{31}P NMR spectra very similar to those of the corresponding Eu^{III} complexes (Figures S4 and S5 in the Supporting Information). This points to a strong preference for a single arrangement around all the phosphorus atoms in complexes of these two phosphinate ligands, in other words the formation of only one of the possible diastereomeric pairs – *RRRR*-Λ-λλλλ (+*SSSS*-Δ-δδδδ) or *SSSS*-Λ-λλλλ (+*RRRR*-Δ-δδδδ). A similar preference for these isomers was observed previously for complexes of H_4DOTP^{Bn} (ref.[16a]) as well as for complexes of tris(phosphinate) monoacetamide cyclen derivatives.[50] Unfortunately, it was not possible to unambiguously determine the absolute configuration of these complexes. The chemical exchange between the major (*RRRR*/*SSSS*) and minor isomers (*RRRS*/*SSSR*) could be demonstrated by the presence of exchange cross-peaks in the two-dimensional exchange (EXSY) NMR spectrum of the $[Yb(DOTP^{H})]^-$ derivative (Figure S8 in the Supporting Information). In addition, the dynamic behaviour of the isomer mixture (by variable-temperature ^{31}P NMR spectra) was also observed in the cases of other ligands (Figure S9 in the Supporting Information).

The ^1H NMR spectra of the Eu^{III} complexes of all ligands (see example in Figure S10 in the Supporting Information) have resonances for the axial protons at δ = 22–32 ppm, which confirms the exclusive presence of the TSA isomer as no signal was observed at the characteristic chemical shifts for axial protons of the SA isomer (above δ = 35 ppm)[17,20,21a,22] The $[Eu(DOTP^{OEt})]^-$, $[Eu(DOTP^{H})]^-$ and $[Eu(DOTP^{OBu})]^-$ complexes have very complex ^1H NMR spectra, thus indicating the presence of many diastereoisomers (a set of resonances was observed for each proton). In contrast, the ^1H NMR spectrum of the $[Eu(DOTP^{hm})]^-$ complex contains a set of eight dominant peaks, which corresponds to the non-equivalent protons of a dominant isomeric species with C_4 symmetry (*RRRR* or *SSSS*), and very weak signals (four for each of the eight types of protons), which correspond to a very minor asymmetric isomer (*RRRS* or *SSSR*, Figure S10, ^1H NMR). A similar situation occurs for the $[Eu(DOTP^{Et})]^-$ complex.

In summary, the ^{31}P and ^1H NMR spectra show the presence of complex diastereomeric mixtures for $[Ln(DOTP^{OEt})]^-$, $[Ln(DOTP^{H})]^-$ and $[Ln(DOTP^{OBu})]^-$ complexes, whereas the $[Ln(DOTP^{hm})]^-$ and $[Ln(DOTP^{Et})]^-$ complexes have a preference for a single configuration.

The solution structures of the H_4DOTP^{OEt}, H_4DOTP^{H} and $DOTP^{OBu}$ complexes can be explained in a similar manner to the complexes of the trifluoroethyl phosphonate monoester derivative.[39] There, the ^{19}F NMR spectra show the presence of all six possible isomers, with the abundances of the *RRRR*/*SSSS* pair slightly higher than, and that of the *RSRS* isomers slightly lower than, the statistical values by a factor of 1.4–1.5. These deviations were interpreted by using a neighbouring interaction model whereby the population differences between the various isomers depend only on the energy difference of the interactions of the substituent groups on neighbouring phosphorus atoms in the *RR* (or *SS*) ($E_{RR} \approx E_{SS}$) and *RS* (or *SR*) ($E_{RS} \approx E_{SR}$) orientations; E_{RS} is smaller than E_{RR} in these compounds by 0.47 kJ mol^{-1}. This small difference should result from a higher steric hindrance between the ester groups and electronic repulsions between the partially charged oxygen atoms in the *RS* orientation. Such a small energy difference could also be present in the complexes of the phosphonate monoester derivatives. The absence of the ester groups should decrease the energy difference between those two interactions, with isomer abundances closer to the statistical distribution.

The preference for a single configuration observed for H_4DOTP^{hm} could be rationalized by hydrogen-bonding interactions between the hydroxy moieties on one phosphorus acid side-chain and the oxygen atoms of the neighbour phosphinate groups. However, such hydrogen bonds are not possible for $[Ln(DOTP^{Et})]^-$ complexes, which also show a strong preference for a single configuration. We can speculate that this isomerism may be a consequence of the electronic properties rather than the steric demands of the substituents on the phosphorus atoms. Thus, ligands in complexes of H_4DOTP^{OEt}, H_4DOTP^{H} and H_4DOTP^{OBu} (and also H_4DOTP^{Ph} and H_4DOTP^{Otfe}),[23,39] which form a mixture of isomers, contain electron-withdrawing substituents and those of H_4DOTP^{Et} and H_4DOTP^{hm} (and also H_4DOTP^{Bn}),[16a] which show a preferential isomerism, have electron-donating alkyl substituents on the phosphorus atoms. The electronic properties could alter the electron distribution inside the PO_2^- moiety and therefore the different preferences for the isomers.

^{17}O and ^{31}P Lanthanide-Induced Shifts

The ^{17}O lanthanide-induced shifts (LISs) were measured for selected complexes, namely the $[Ln(DOTP^{hm})]^-$ complexes as representatives of the group of compounds with a dominant diastereoisomer (*RRRR*/*SSSS*) and the

$[Ln(DOTP^{OEt})]^-$ and $[Ln(DOTP^{H})]^-$ complexes as representatives of the other group which shows no preference for either of the possible isomeric forms.

The LIS (Δ, the lanthanide-induced shift for a concentration of 1 M of Ln^{III} ion)[51] consists of diamagnetic (Δ_d), contact (Δ_c) and pseudocontact (Δ_p) contributions [Equation (1)].

$$\Delta = \Delta_d + \Delta_c + \Delta_p \quad (1)$$

The paramagnetic contribution to the LIS, Δ', obtained after subtraction of the diamagnetic term, Δ_d, can be expressed as Equation (2), which contains terms that are characteristic of each lanthanide(III) ion but independent of the ligand ($<S_z>$ and C^D for Δ_c and Δ_p, respectively) and characteristic of the nucleus under study but independent of the lanthanide(III) cation (F and G for Δ_c and Δ_p, respectively).

$$\Delta' = q(<S_z> \times F + C^D \times G) \quad (2)$$

Equation (2) can be linearized to obtain either qF in the contact contribution from the slope of the plot obtained from Equation (3) or the geometric term qG in the pseudocontact contribution from the slope of the plot corresponding to Equation (4).

$$\Delta'/C^D = (<S_z>/C^D) \times qF + qG \quad (3)$$

$$\Delta'/<S_z> = qF + (C^D/<S_z>) \times G \quad (4)$$

Equation (3) is best used to study nuclei with a dominant contact contribution, such as the ^{17}O nucleus of the water oxygen atom directly bound to the central lanthanide(III) ion in the complexes with inner-sphere water, whereas Equation (4) is preferably used to study nuclei where the pseudocontact contribution dominates, usually those nuclei lacking any direct bonding to the central lanthanide(III) ion, which in the present case is the phosphorus atoms. When the series of lanthanide(III) complexes with a particular ligand are isostructural, the plots obtained from Equations (3) and (4) are straight lines.

Analysis of the ^{17}O LIS data for the Ln^{III} complexes of H_4DOTP^H, H_4DOTP^{hm} and H_4DOTP^{OEt} according to Equations (3) and (4) is shown in Figure 5. Data for the complexes of H_8DOTP are also given for comparison. The data for the complexes of H_4DOTP^{hm} show a linear trend across the lanthanide series, which indicates that these complexes are isostructural. The slope (qF) of the plot according to Equation (3) is –30, and since the value of F is around –90 under the conditions applied,[51] this gives q value of around 0.3. A comparable value was obtained by luminescence lifetime measurements on Eu^{III} complexes. However, combining these results with the UV/Vis study, which clearly showed the presence of a single coordination structure, suggests that q is actually 0. The relatively small negative slope is probably due to the presence of water in the second coordination sphere.

The plots for the lanthanide complexes of the other ligands deviate from linearity towards more negative values for one or more of the lighter lanthanides (Ce^{III} for H_4DOTP^H and H_4DOTP^{OEt}; Ce^{III}, Pr^{III}, and Nd^{III} for H_8DOTP).[51] The line through the data according to Equation (3) for Ce^{III}, Pr^{III} and Nd^{III} complexes of H_8DOTP has a slope (qF) of –80, which indicates that these light lanthanides form complexes of H_8DOTP with one water molecule in the first coordination sphere of the lanthanide(III) ions. The large negative values of Δ'/C^D for the Ce^{III} complexes of H_4DOTP^H and H_4DOTP^{OEt} suggest that these complexes contain the water molecule in the first coordination sphere as well. The plots obtained from Equation (4) (Figure 5), where the points corresponding to the Ce^{III} complexes of H_4DOTP^H and H_4DOTP^{OEt} and those for the Ce^{III}, Pr^{III} and Nd^{III} complexes of H_8DOTP lie significantly far from the linear fits, support this conclusion.

The negative sign of the slope of the plots obtained from Equation (4) for the lanthanide(III) complexes of H_4DOTP^{hm} is rather surprising when compared with those observed for the other ligands (Figure 5). As such slopes are proportional to the geometric term G of the ^{17}O nuclei of the water molecules, a change in the sign of the slope could be a consequence of a different spatial orientation of the second-sphere hydration shell around the lanthanide(III) complexes of H_4DOTP^{hm} in comparison with the complexes of the other ligands. As all the ligands are symmetrical, the main magnetic axis of their lanthanide(III) complexes should have the same direction as their pseudo-C_4 axis. Thus, the sign of the ^{17}O G value is given by the spatial location of the second-sphere water molecules relative to the dipolar cone defined by the "magic" angle θ = 54.7° which cancels out the geometric term $G = (3 \times \cos^2\theta - 1)/r^3$, where θ is the angle between the main magnetic axis of the complex and the line connecting the ion with the ^{17}O nucleus at distance r. When these water molecules pass from the inside to the outside part of the cone, the sign of G and of the corresponding pseudocontact shift is reversed. The value of G is positive inside the cone, whereas it is negative outside. The second-sphere water molecules are therefore located outside of the dipolar cone in the H_4DOTP^{hm} complexes, whereas for H_4DOTP^H, H_4DOTP^{OEt} and H_8DOTP they are inside this cone (Figure S11 in the Supporting Information).

These findings suggest that all alkyl groups in the complexes of H_4DOTP^{hm} and H_4DOTP^{Et} are oriented above the O_4-plane, thus avoiding an approach of the water molecule inside the cone. This is supported by the crystal structures of several lanthanide(III) complexes with H_4DOTP^{Bn}, in which all benzylic groups are directed above the O_4-plane to form a hydrophobic cavity. This arrangement leads exclusively to *RRRR*-Λ-λλλλ + *SSSS*-Δ-δδδδ enantiomeric pairs in the solid state, and these complexes are also present in the solution as the single isomer.[16] It is also supported by the high stability of the symmetric arrangement, as evidenced by the relatively high interconversion energy between isomers of $[Yb(DOTP^{hm})]^-$ compared to more labile

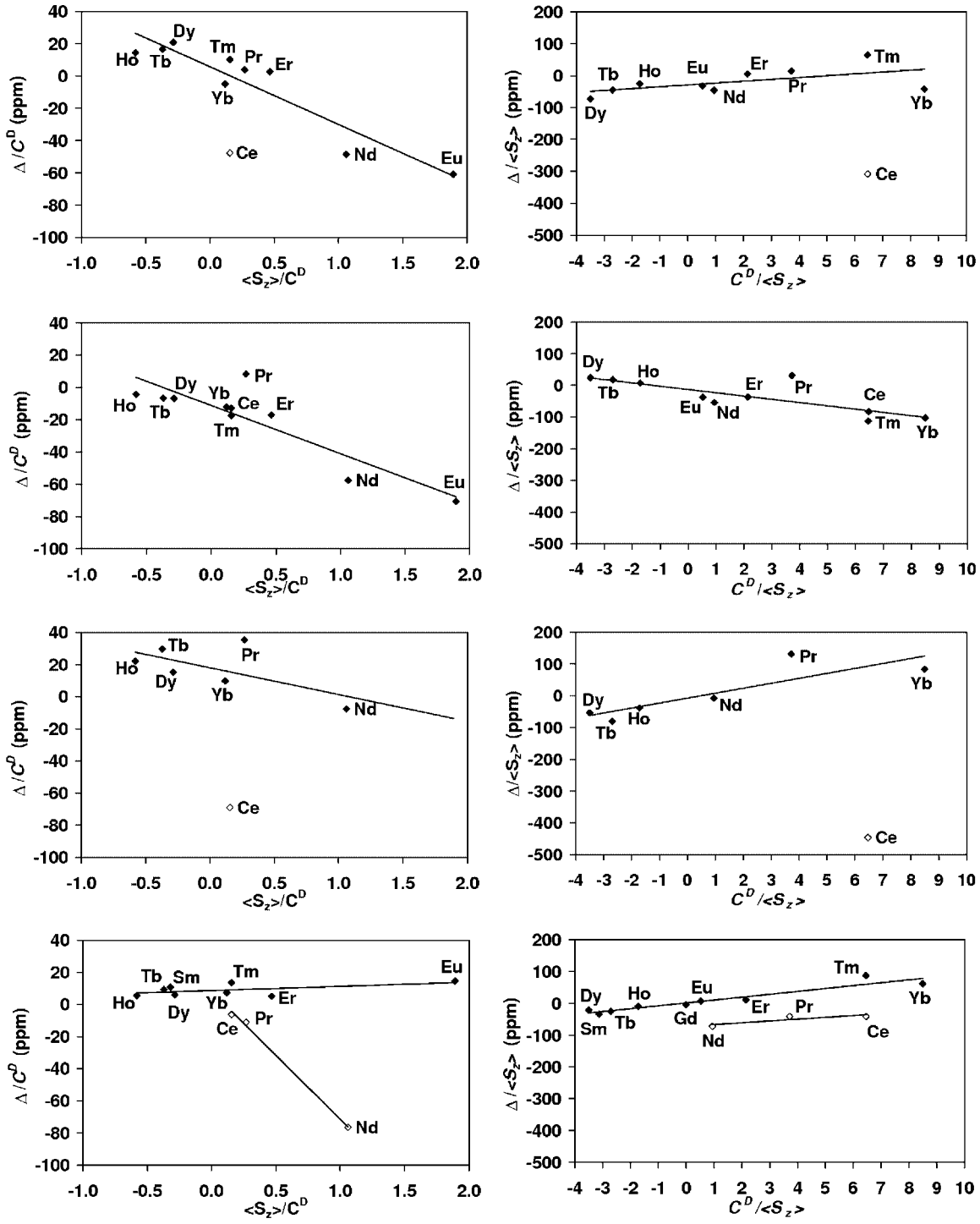

Figure 5. Linearization of the ^{17}O LIS data for the lanthanide(III) complexes of H_4DOTP^H (top), H_4DOTP^{hm} (center top), H_4DOTP^{OEt} (center bottom) and H_8DOTP (bottom) according to Equations (3) (slope = contact shift, left) and (4) (slope = pseudocontact shift, right); T = 301 K, pH 7.

[Yb(DOTP^{OEt})]$^-$ (see the variable-temperature ^{31}P NMR spectra in Figure S9 of the Supporting Information).

Similar equations can be derived for the ^{31}P NMR LIS values [q in Equations (3) and (4) should be replaced by 1]. In the case of [Ln(DOTP^{hm})]$^-$ and [Ln(DOTP^{Et})]$^-$ complexes, the ^{31}P LIS values for [Ln(DOTP^{hm})]$^-$ and [Ln(DOTP^{Et})]$^-$ were determined for the major *RRRR* (*SSSS*) isomer as its signal can easily be assigned in the spectra (Figure 6). The plots obtained from Equations (3) and (4) clearly show a break between the first and second half of the Ln series, thus indicating a non-isostructurality of these complexes across the lanthanide series. The com-

plex isomeric mixtures present for the $[Ln(DOTP^{H})]^{-}$, $[Ln(DOTP^{OEt})]^{-}$ and $[Ln(DOTP^{OBu})]^{-}$ complexes do not allow a reliable assignment of the resonances, therefore the weighted average of the chemical shifts for all isomers (i.e. the chemical shift corresponding to half of the total intensity of all signals in the ^{31}P NMR spectra) was used. The corresponding plots are very similar to the previous case {the data for $[Ln(DOTP^{H})]^{-}$ are included in Figure 6}. Analogous ^{31}P LIS phenomena have also been observed previously for Ln^{III} complexes of H_4DOTP^{Ph} and H_4DOTP^{Bn}.[15,16]

The positions of the breaks observed in the plots of the ^{31}P NMR spectroscopic data do not fully correspond with those observed in the ^{17}O NMR spectroscopic data, poss-

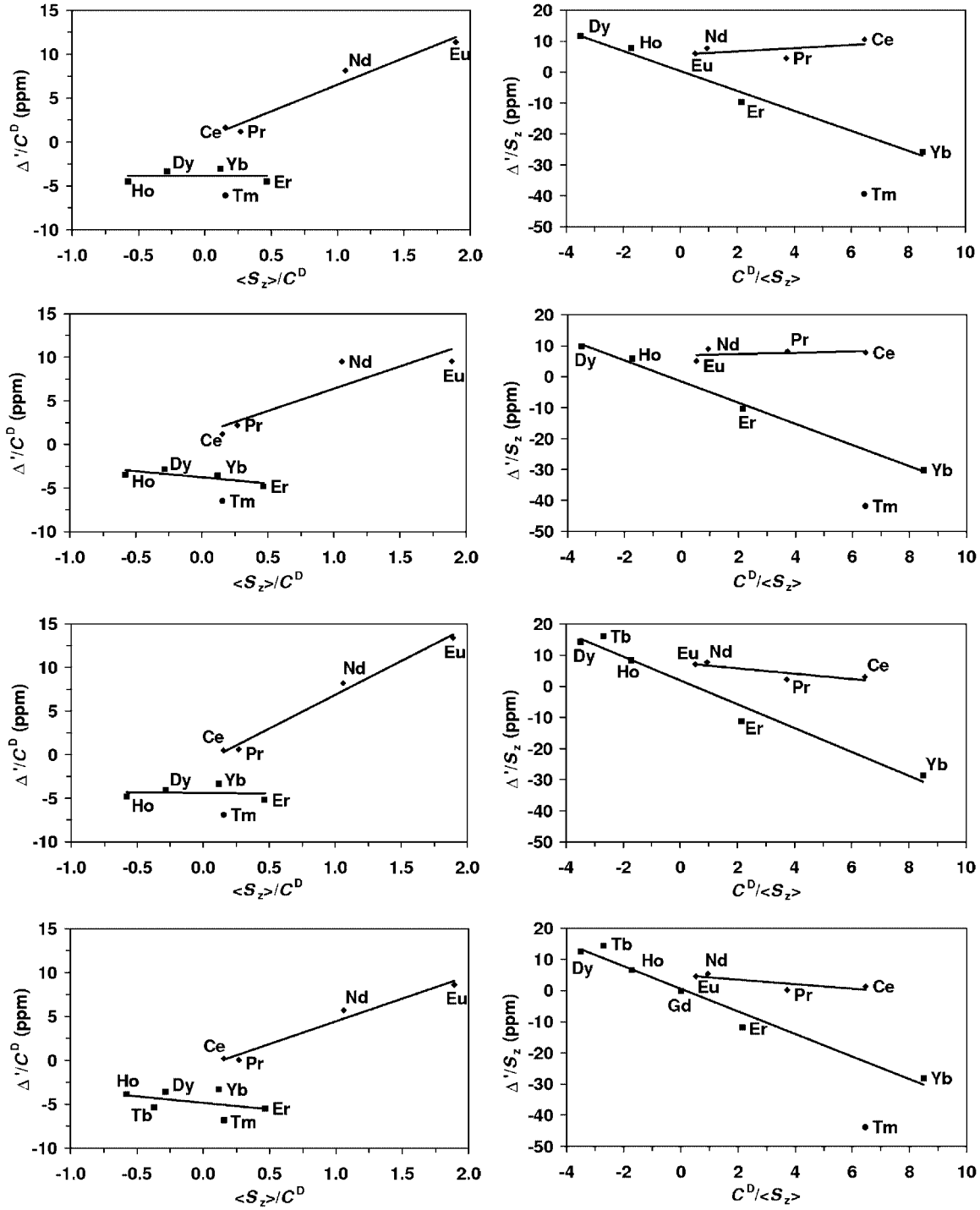

Figure 6. Separation of the contact [Equation (3), left] and pseudocontact [Equation (4), right] contributions to the ^{31}P LIS for the weighted chemical shift for the $[Ln(DOTP^{H})]^{-}$ complexes (top), the *RRRR* (*SSSS*) isomers of the $[Ln(DOTP^{hm})]^{-}$ (center top) and $[Ln(DOTP^{Et})]^{-}$ (center bottom) complexes, and $[Ln(H_{1.5}DOTP)]^{3.5-}$ (bottom); T = 301 K, pH 7.

ibly due to a change in the water coordination of the lanthanide ions. Since the breaks in Figure 6 indicate a change of both *F* and *G* for the ^{31}P nuclei of these complexes across the lanthanide series, it is highly likely that some geometric change in the TSA coordination sphere is occurring. The ions along the lanthanide(III) series gradually move inside the ligand cavity (closer to the N_4-plane) in the TSA isomers – the Ln–QN distance (QN is the centre of gravity of the N_4-plane) drops steeply from around 1.85 Å for La^{III} to around 1.65 Å for Eu^{III}, and remains in the range 1.65–1.55 Å for the rest of the series.[23,37] This leads to a change of geometry of the donor atom environment between large (La^{III}–Eu^{III}) and small (Eu^{III}–Lu^{III}) ions, which is apparently reflected in changes of both *F* and *G* for the ^{31}P nuclei.

Relaxometric and EPR Measurements

Variable-temperature ^{17}O NMR spectroscopic data [T_1 and T_2 relaxation times and ^{17}O angular frequencies (ω_O)] were collected for the Gd^{III} complexes of H_4DOTP^{hm}, H_4DOTP^{H} and H_4DOTP^{OEt}. For comparative purposes,

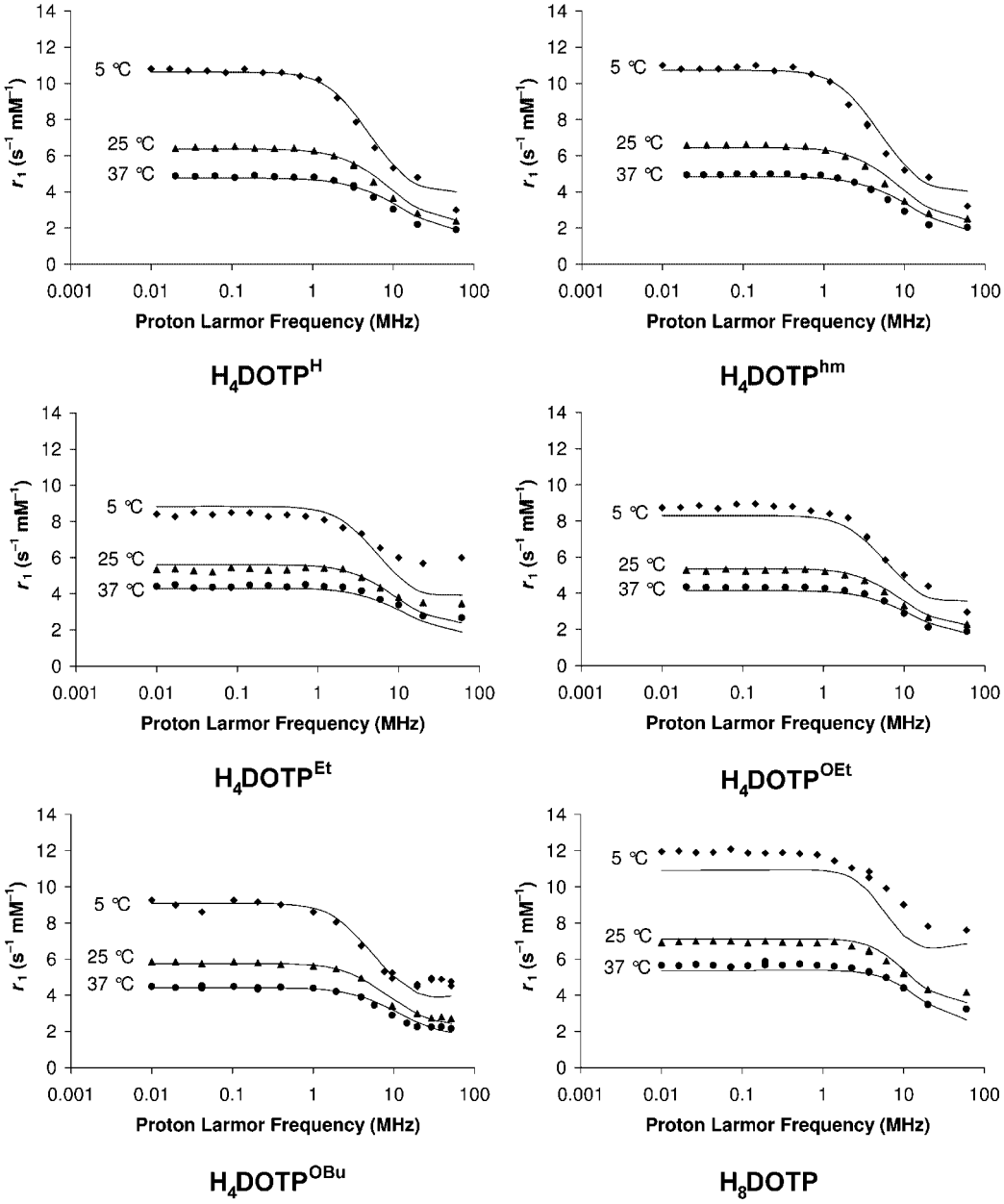

Figure 7. The ^1H NMRD profiles for the Gd^{III} complexes of H_4DOTP^{H}, H_4DOTP^{hm}, H_4DOTP^{Et}, H_4DOTP^{OEt}, H_4DOTP^{OBu} and H_4DOTP. Profiles were measured at pH 7 (except for H_8DOTP) and 10 (H_8DOTP). The full lines represent the results of the best simultaneous fits of ^1H NMRD and EPR data.

the data for the $[Gd(DOTP)]^{5-}$ complex were also measured at a pH of around 10 (where all pendant arms are fully deprotonated) and a pH of about 7 {where approximately 1.5 protons are bound to the ligand, i.e. $[Gd(H_{1.5}DOTP)]^{3.5-}$[44]}. In this case, no significant influence of the pH on the data obtained was observed. The ^{17}O NMR spectroscopic data are shown in Figure S12 (see the Supporting Information). Since $q = 0$ for these systems, the paramagnetic effects on the ^{17}O NMR parameters are so small that a fitting to theoretical models is not feasible.

The ^1H NMRD profiles of the Gd^{III} complexes of H_4DOTP^H, H_4DOTP^{hm}, H_4DOTP^{Et}, H_4DOTP^{OEt}, H_4DOTP^{OBu} and H_8DOTP at 5, 25 and 37 °C are shown in Figure 7. The Gd^{III} complexes of H_4DOTP^{Et}, H_4DOTP^{OEt} and H_8DOTP were re-measured, and the published ^1H NMRD profile for the H_4DOTP^{OBu} complex[13] was used. These profiles were re-analysed as the second-sphere hydration was not considered in previous relaxometric studies.[13] The values of the r_1 relaxivities of phosphinates and phosphonate monoesters are about half those measured for $[Gd(H_2O)(DOTA)]^-$; for example, the relaxivity at 20 MHz and 310 K is about 2.1 $s^{-1}mm^{-1}$ for all these complexes (Table 6). The ^1H NMRD profiles of the $[Gd(DOTP^H)]^-$ and $[Gd(DOTP^{hm})]^-$ complexes are similar to each other, in contrast to those of the $[Gd(DOTP^{Et})]^-$, $[Gd(DOTP^{OEt})]^-$ and $[Gd(DOTP^{OBu})]^-$ complexes, which have significantly lower relaxivities at low fields. As all these complexes have approximately the same molecular size, these differences can be attributed to a slower electronic spin relaxation and/or to a somewhat higher polarity of the H_4DOTP^H and H_4DOTP^{hm} complexes in comparison to the other complexes, which can lead to a richer second hydration sphere in the former complexes.

To obtain more information about electronic parameters, transverse electronic spin relaxation times ($T_{2e,exp}$) were calculated from the peak-to-peak EPR line widths (ΔH_{pp}) according to Equation (5), where g_L is the Landé g factor (Table 5).[52] The ^1H NMRD data were then fitted simultaneously with the X-band EPR data by using a set of equations suitable for complexes with an extended second hydration sphere.[22,27b]

$$T_{2e,exp} = \frac{h}{\pi \times g_L \times \beta \times \Delta H_{pp} \times \sqrt{3}} \quad (5)$$

Since the number of parameters in these equations is rather large, and some of them correlate strongly, we fixed many of them. The diffusion coefficients of the various complexes were fixed at values obtained by a semi-empirical method from their molecular weights, and the corresponding activation energy was fixed at 18.2 kJ mol^{-1}.[53] The shortest distance of a water proton to the Gd^{III} nucleus (the closest approach, a_{GdH}) was fixed at 3.50 Å, the same value as in most previous studies. The water molecules in the second coordination sphere are assumed to be hydrogen-bonded to the Gd^{III}-coordinated O-atoms of the ligands. Accordingly, the effective distance between Gd^{III} and these protons (R_{GdH}) was fixed at 3.6 Å. The residence time of the second-sphere water molecules ($\tau_{M,ss}$) was taken as 56 ps, the value calculated by Borel et al. for $[Gd(DOTP)]^{5-}$ by molecular dynamics, and the corresponding activation energy was fixed at 35 kJ mol^{-1}.[29] The rotational correlation times (τ_R) were estimated from the previously evaluated correlation time for $[Gd(H_2O)(DOTA)]^-$ after application of a correction for the molecular volume by means of the Stokes–Debye–Einstein equation, and the activation energy for this correlation time was fixed at 25.4 kJ mol^{-1} for all complexes. Only q_{ss}, the mean-square zero-field splitting energy (Δ^2) and the correlation time for the modulation of the zero-field splitting interaction (τ_v) remained as adjustable parameters in the fitting procedure. The activation energy of the latter parameter was fixed to a reasonable value of 1 kJ mol^{-1} because fittings with this as a variable parameter led to negative values. Inclusion of the ^1H NMRD profiles measured at 5 °C resulted in very unreasonable values of Δ^2 and τ_v, therefore these profiles were given zero weight in the fittings.

The best values of the adjustable parameters for the Gd^{III} complexes of these ligands are given in Table 6. The values of $T_{2e,exp}$ (from EPR data) and $T_{2e,calc}$, calculated by using the best-fit parameters τ_v and Δ^2, are in good agreement (Table 5). The calculated ^1H NMRD profiles are represented by the curves in Figure 7.

The values of the electronic parameters τ_v and Δ^2 could not be determined accurately from the ^1H NMRD profiles, although the profiles appeared to be very sensitive to the value of q_{ss}. The best-fit parameters obtained (Table 6) also support the preliminary conclusion made above, namely that the $[Gd(DOTP^H)]^-$ and $[Gd(DOTP^{hm})]^-$ complexes have a slower electronic spin relaxation and a somewhat richer second hydration sphere than the $[Gd(DOTP^{Et})]^-$, $[Gd(DOTP^{OEt})]^-$ and $[Gd(DOTP^{OBu})]^-$ complexes (see also the luminescence measurements). As expected, the highest second-sphere hydration was found in the case of $[Gd(DOTP)]^{5-}$. The values for Δ^2 are an order of magnitude larger than that for $[Gd(H_2O)(DOTA)]^-$, which may attributed to the lower rigidity of the complexes of H_4DOTP^R

Table 5. Experimental ($1/T_{2e,exp}$, calculated from EPR ΔH_{pp}) and calculated ($1/T_{2e,fit}$, simultaneous fitting of ^1H NMRD and EPR data) $1/T_{2e}$ values for the Gd^{III} complexes.

Parameter	$[Gd(DOTP^H)]^-$	$[Gd(DOTP^{hm})]^-$	$[Gd(DOTP^{Et})]^-$	$[Gd(DOTP^{OEt})]^-$	$[Gd(DOTP^{OBu})]^-$	$[Gd(DOTP)]^{5-}$	$[Gd(H_2O)(DOTA)]^-$
ΔH_{pp} [Gauss]	275 ± 5	280 ± 5	415 ± 2	425 ± 5	362 ± 16	605 ± 10	91[a]
$1/T_{2e,exp}$ [10^9 s^{-1}][b]	4.19	4.27	6.33	6.40	5.49	9.22	1.40
$1/T_{2e,fit}$ [10^9 s^{-1}]	4.19	4.27	6.33	6.40	5.49	9.25	–

[a] Ref.[3] [b] Values calculated according to Equation (5).

Table 6. Results of multi-parameter simultaneous fitting of ^1H NMRD and EPR data for Gd^{III} complexes of the H_4DOTP^R derivatives (at pH 7) and H_8DOTP (at pH 10). The values in italics were fixed during the fitting.

Parameter	$[Gd(DOTP^H)]^-$	$[Gd(DOTP^{hm})]^-$	$[Gd(DOTP^{OEt})]^-$	$[Gd(DOTP^{OBu})]^-$	$[Gd(DOTP^{Et})]^-$	$[Gd(DOTP)]^{5-}$	$[Gd(H_2O)(DOTA)]^-$
$^{310}r_{1,exp}$ [$s^{-1}mm^{-1}$]	2.2[a]	2.2[a]	2.1[a]	2.3[a]	2.8[a]	3.5[a]	3.8[b]
$^{310}r_{1,calc}$ [$s^{-1}mm^{-1}$]	2.6[c]	2.6[c]	2.4[c]	2.5[c]	2.5[c]	3.5[c]	4.4[d]
$^{310}r_{1os,calc}$ [$s^{-1}mm^{-1}$]	2.1[e]	2.1[e]	2.1[e]	2.2[e]	2.1[e]	2.1[e]	2.4[f]
$^{310}r_{1ss,calc}$ [$s^{-1}mm^{-1}$]	0.5[g]	0.5[g]	0.3[g]	0.4[g]	0.3[g]	1.4[g]	0[h]
q_{ss}	1.32 ± 0.05	1.22 ± 0.06	0.68 ± 0.04	0.80 ± 0.04	0.79 ± 0.06	3.3 ± 0.1	0
$^{298}\tau_R$ [ps]	*86.6*[i]	*106.0*[i]	*127.1*[i]	*162.0*[i]	*117.3*[i]	*90.7*[i]	*77*[j]
$^{298}\tau_v$ [ps]	2.7 ± 1.7	2.6 ± 2.0	3.8 ± 1.3	4.8 ± 1.1	5.0 ± 4.6	12.7 ± 0.2	11[j]
Δ^2 [10^{20} s^{-2}]	1.4 ± 0.8	1.5 ± 1.0	1.6 ± 0.5	1.1 ± 0.2	1.0 ± 0.8	0.9 ± 0.1	0.16[j]
$^{298}\tau_{S0}$ [ps][k]	220	214	137	158	157	73	473
$^{298}D_{GdH}$ [10^{-9} m^2s^{-1}][l]	*2.48*	*2.40*	*2.37*	*2.33*	*2.38*	*2.43*	–

[a] Experimental relaxivity values as measured at 310 K and 20 MHz. [b] Ref.[54], 312 K. [c] Relaxivity at 310 K and 20 MHz as calculated with the best-fit parameters reported in this paper. [d] Relaxivity at 310 K and 20 MHz as calculated with the best-fit parameters reported in ref.[54] [e] Outer-sphere contribution to relaxivity at 310 K and 20 MHz as calculated with the best-fit parameters reported in this paper. [f] Outer-sphere contribution to relaxivity at 310 K and 20 MHz as calculated with the best-fit parameters reported in ref.[54] [g] Second-sphere contribution to relaxivity at 310 K and 20 MHz as calculated with the best-fit parameters reported in this paper. [h] Second-sphere contribution to relaxivity at 310 K and 20 MHz as calculated with the best-fit parameters reported in ref.[54] [i] Calculated using a molecular volume as evaluated with HyperChem® and the Stokes–Debye–Einstein equation. [j] Ref.[54] [k] Low field limiting value of the electronic relaxation correlation time as calculated with $\tau_{S0} = (12\Delta^2\tau_v)^{-1}$. [l] Calculated from the molecular weight using a previously reported equation.[52]

and H_8DOTP due to the lack of an inner-sphere water molecule, which leads to larger deformation of the complexes upon collision with solvent molecules. As a result, the electronic relaxation rates of the presently studied complexes are lower than that of $[Gd(H_2O)(DOTA)]^-$ (ref.[54]), which means that the outer-sphere contribution to the relaxivity of these complexes is somewhat lower. The second-sphere water molecules {except for $[Gd(DOTP)]^{5-}$ complex} have a contribution of 10–20% to the total relaxivity (Table 6).

The pH-dependence of the relaxivity of the Gd^{III} complexes in solution was also examined. No protonation of the pendant arms is expected above a pH of around 3 for phosphinic acid or phosphonic monoester groups as they are highly acidic (see above),[37] therefore no pH dependence was expected. Surprisingly, the relaxivity of the $[Gd(DOTP^{hm})]^-$ complex was found to be highly dependent on the pH, in sharp contrast to the relaxivities of other complexes, which were found to be independent of the pH (tested at pH 4, 7 and 10). The relaxivity of the $[Gd(DOTP^{hm})]^-$ complex increases by more than 50% upon going from neutral to both acidic and alkaline pH regions (Figure S13 in the Supporting Information). This observation can be explained by a prototropic exchange similar to that observed for the Gd^{III} complexes of H_4DOTA amides.[46] In the strongly acid region (pH < 2), a partial decomplexation probably takes place leading to a further relaxivity increase.

Conclusions

We have synthesized and studied a series of tetraphosphorus acid ligands and, in particular, their complexes with Ln^{III} ions. These ligands and their complexes were characterized by several methods in order to gain insight into their stabilities and structures. The ligands are less basic than the parent system H_4DOTA and, consequently, the Gd^{III} complexes are thermodynamically much less stable. Titrations have shown that there is no (de)protonation of the preformed complexes in the pH range 3–10. Luminescence data do not allow an unambiguous conclusion regarding the value of q for the Eu^{III} complexes of the tetraphosphorus acid derivatives as the measured lifetimes suggest q valus of around 0.5. However, UV/Vis measurements on the Eu^{III} complexes confirm that heavier lanthanide(III) complexes lack an inner-sphere water molecule.

This finding was confirmed by the X-ray structures of the Gd^{III} complexes. Exclusive formation of the TSA isomer was observed by both multinuclear NMR spectroscopy and by X-ray diffraction. The presence of inner-sphere coordinated water was found only for the $[Ce(H_2O)(DOTP^H)]^-$, $[Ce(H_2O)(DOTP^{OEt})]^-$ and $[Ln(H_2O)(DOTP)]^{5-}$ (Ln = Ce, Pr, Nd) complexes through the measurements of ^{17}O lanthanide-induced shifts. The ^{31}P NMR study revealed striking differences in isomerism between the $[Ln(DOTP^{hm})]^-$ and $[Ln(DOTP^{Et})]^-$ complexes on the one hand and the $[Ln(DOTP^H)]^-$, $[Ln(DOTP^{OEt})]^-$ and $[Ln(DOTP^{OBu})]^-$ complexes on the other. Thus, whereas rich isomeric mixtures were found in the latter cases, the $[Ln(DOTP^{hm})]^-$ and $[Ln(DOTP^{Et})]^-$ complexes show a clear preference for the *RRRR*/*SSSS* arrangement on the phosphorus atoms, although they probably form *RRRR*-Λ-λλλλ + *SSSS*-Δ-δδδδ enantiomeric pairs similar to those found previously in the case of $[Ln(DOTP^{Bn})]^-$ complexes.[16] This is probably caused by a strong interaction of the side-chains in the preferential arrangement.

To explore the second-hydration sphere in more detail, a relaxometric study on all the Gd^{III} complexes was also performed. The ^1H NMRD and EPR data were fitted simultaneously, and the best-fit parameters suggest that about three second-sphere water molecules are present in the case of $[Gd(DOTP)]^{5-}$ and about one second-sphere

water molecule is present in the other complexes. The electronic spin relaxation parameters τ_v and Δ^2 obtained suggest that the more hydrophilic $[Gd(DOTP^{H})]^{-}$ and $[Gd(DOTP^{hm})]^{-}$ complexes have a slower electronic spin relaxation and a somewhat richer second hydration sphere than the $[Gd(DOTP^{Et})]^{-}$, $[Gd(DOTP^{OEt})]^{-}$ and $[Gd(DOTP^{OBu})]^{-}$ complexes. The pH-dependence of the relaxivity observed for the $[Gd(DOTP^{hm})]^{-}$ complex reflects the proton/hydroxide catalysis of the prototropic exchange mechanism, similar to that observed for the Gd^{III} complexes of H_4DOTA amides.[46]

The observed relaxivities of all $[Gd(DOTP^{R})]^{-}$ complexes fall into the narrow region 2.1–2.8 s^{-1} mM^{-1} (20 MHz, 37 °C). The relaxivity of Gd^{III} complexes with DOTA-like ligands having one inner-sphere water molecule is higher (≈ 4),[22,54] although in these cases the inner-sphere contributions are about 50% of the final value, whereas the second-sphere water molecules of the presently studied complexes have a contribution of only 10–15% to the total relaxivity. The ligands studied differ in the size and hydrophilic/hydrophobic character of the substituents on the phosphorus atoms and in the isomeric distributions of their complexes in solution. However, this has only a marginal influence on the relaxivity. This indicates that the second-sphere water molecules contributing to the relaxivity (i.e. residing close to the central Gd^{III} ion) are mainly connected with the oxygen atoms of electronegative PO_2^- moiety through hydrogen bonds, independently on the orientation of the side chains and, consequently, on the local arrangement of the second-sphere water molecules.

Experimental Section

General: Cyclen (1,4,7,10-tetraazacyclododecane, Strem or CheMa-Tech), hypophosphorous acid (Fluka), triethyl phosphite (Fluka), $LnCl_3$ hydrates (Strem or Aldrich), D_2O (99.95%D, Chemtrade) and Dowex 50 (×4, 100–200 mesh, Fluka) were used without further purification. Paraformaldehyde was filtered from an old formaldehyde solution and dried over P_2O_5 in vacuo. Anhydrous EtOH was obtained from Lachema (Czech Republic). H_4DOTP^{Et} and H_4DOTP^{OBu} were synthesized according to literature procedures.[13,33] ^{1}H (400 MHz), ^{13}C (101 MHz) and ^{31}P (162 MHz) NMR spectra were recorded with a Varian INOVA 400 spectrometer in $CDCl_3$, D_2O or H_2O solutions at 25 °C, or with a Varian Unity 500 spectrometer (^{1}H: 499.82 MHz; ^{31}P: 202.33 MHz). For measurements in D_2O, the internal standard was *t*BuOH; in $CDCl_3$, the internal standard was TMS; for ^{31}P, 85% H_3PO_4 was used as an external standard. The elemental analyses were carried out at the Institute of Macromolecular Chemistry (Academy of Sciences of the Czech Republic, Prague). Luminescence measurements were performed with an Aminco Bowman® Series 2 spectrometer by using the excitation at the $^5L_6 \leftarrow {}^7F_0$ band (396 nm). Emission lifetimes were measured for the $^7F_2 \leftarrow {}^5D_0$ transition (615 and 621 nm). In general, the samples prepared for NMR measurements were also used for luminescence measurements. UV/Vis spectra of the $^5D_0 \leftarrow {}^7F_0$ transition were acquired with a Perkin–Elmer Lambda 19 spectrometer, in data steps of 0.01 nm. The concentration of the samples was around 0.02 M.

1,4,7,10-Tetraazacyclododecane-1,4,7,10-tetrakis(methylphosphinic acid) (H_4DOTP^{H}): Cyclen (1.00 g, 5.80 mmol) and 50% aqueous hypophosphorous acid (7.2 mL, 66 mmol) were mixed in water (20 mL). The mixture was heated to 40 °C whilst being stirred, and solid paraformaldehyde (0.78 g, 26 mmol) was added in small portions over 60 min. The mixture was further heated at this temperature for 1 d. Excess paraformaldehyde was then filtered off. After concentration to a small volume under reduced pressure, the reaction mixture was purified on a cation exchange resin (Dowex 50, H^+-form, 300 mL, elution with water). Phosphinic acid and other acidic impurities were eluted first followed by the product. Fractions containing the pure ligand (checked by ^{31}P NMR) were combined and concentrated in vacuo. Microcrystallinic $H_4DOTP^{H}\cdot 0.5H_2O$ (0.66 g, 23%) was obtained after slow evaporation of the solvent from an aqueous ligand solution. ^{1}H NMR (D_2O): δ = 2.53–2.55 (m, $^2J_{P,H}$ = 8.8 Hz, 24 H, CH_2P, NCH_2CH_2N), 7.04 (d, $^1J_{P,H}$ = 504.0 Hz, 4 H, PH) ppm. ^{31}P NMR (D_2O): δ = 22.5 (dt, $^1J_{P,H}$ = 504, $^2J_{P,H}$ = 9.2 Hz) ppm. $^{31}P\{^1H\}$ NMR (D_2O): δ = 22.5 (s) ppm. $C_{12}H_{32}N_4O_8P_4\cdot 0.5H_2O$ (493.31): calcd. C 29.22, H 6.74, N 11.36; found C 29.29, H 6.62, N 11.38.

1,4,7,10-Tetraazacyclododecane-1,4,7,10-tetrakis[(hydroxymethyl)-(methyl)phosphinic acid] (H_4DOTP^{hm}): Paraformaldehyde (0.93 g, 31 mmol) was added to an aqueous solution of H_4DOTP^{H} hydrate (1.00 g, 2.03 mmol), and the mixture was stirred and heated under reflux for 1 d. The mixture was then concentrated to dryness under reduced pressure and redissolved in a small amount of water. The solution was purified on a cation exchange column (Dowex 50, H^+-form, 300 mL, elution with water). The first fractions containing the product were combined, and the solvent was evaporated. The residue was dissolved in a small amount of water, and the product was precipitated by addition of acetone. The solid was filtered off and dried with P_2O_5. A white microcrystalline solid was isolated in 51% yield (0.65 g). ^{1}H NMR (D_2O): δ = 2.70–2.60 (m, 24 H, CH_2OH, NCH_2CH_2N), 3.46 (d, $^2J_{P,H}$ = 5.6 Hz, 8 H, NCH_2P) ppm. $^{31}P\{^1H\}$ NMR (D_2O): δ = 38.2 (s) ppm. $C_{16}H_{40}N_4O_{12}P_4\cdot 1.5H_2O$ (631.43): calcd. C 30.44, H 6.86, N 8.87; found C 30.50, H 6.68, N 8.66.

Monoethyl 1,4,7,10-Tetraazacyclododecane-1,4,7,10-tetrakis-(methylphosphonate) (H_4DOTP^{OEt}):[32] Cyclen (1.00 g, 5.80 mmol) was treated with paraformaldehyde (0.87 g, 29 mmol) and triethyl phosphite (9.8 g, 59 mmol, as solvent) to produce the octaethyl ester Et_8DOTP. The mixture was stirred at 40 °C for 3 d and then loaded onto a cation exchange column (Dowex 50, H^+-form, 300 mL). Di- and triethyl phosphite were eluted with EtOH, and Et_8DOTP was washed out with a 1:3 (v:v) mixture of 25% aq. NH_3/EtOH. The fractions containing the desired ester were concentrated in vacuo, after which the purity and the identity of this compound was verified by NMR spectroscopy [^{1}H NMR ($CDCl_3$): δ = 1.27 (t, $^3J_{H,H}$ = 7.2 Hz, 24 H, CH_3), 2.82 (s, 16 H, NCH_2CH_2N), 2.94 (d, $^2J_{P,H}$ = 9.2 Hz, 8 H, NCH_2P), 4.03–4.11 (m, 16 H, OCH_2) ppm. ^{13}C NMR ($CDCl_3$): δ = 16.5 s (CH_3), 50.6 (d, $^1J_{C,P}$ = 151.5 Hz, NCH_2P), 53.4 (s, NCH_2CH_2N), 61.5 (s, OCH_2) ppm. $^{31}P(^1H)$ NMR ($CDCl_3$): δ = 26.7 (s) ppm. The target ligand was obtained after hydrolysis (1 d, 50 °C) of this ester in aq. NaOH (10%, 25 mL). The sodium ions were completely removed by passing the reaction mixture through a cation exchange resin (Dowex 50, H^+-form, 300 mL, elution with water). Evaporation of the water from the eluate resulted in a colourless oil. The ligand was obtained as a white microcrystalline solid after precipitation from its aqueous solution by slow addition of acetone, filtering and drying over P_2O_5 (3.91 g, 92% based on cyclen). ^{1}H NMR (D_2O): δ = 1.18 (t, $^3J_{H,H}$ = 6.8 Hz, 12 H, CH_3), 3.20–3.27 (m, 24 H, NCH_2P, NCH_2CH_2N), 3.89–3.96 (m, 8 H, OCH_2) ppm. $^{31}P\{^1H\}$ NMR (D_2O): δ = 19.4 (s) ppm. $C_{20}H_{48}N_4O_{12}P_4\cdot 4H_2O$ (732.57): calcd. C 32.79, H 7.70, N 7.65; found C 32.65, H 6.94, N 7.63.

1,4,7,10-Tetraazacyclododecane-1,4,7,10-tetrakis(methylphosphonic acid) (H_8DOTP): The target ligand was obtained after acid hydrolysis (aq. HCl 1:1, 2 d, reflux) of the ester obtained as above. The reaction mixture was concentrated, and the residue was recrystallized from boiling water. The ligand, in the form of a white microcrystalline solid, was collected by filtration and dried in air (95% based on cyclen). Spectroscopic data were identical with those reported in the literature.[35] $C_{12}H_{32}N_4O_{12}P_4 \cdot 1.5H_2O$ (575.33): calcd. C 25.05, H 6.13, N 9.74; found C 25.01, H 6.04, N 9.78.

Lanthanide(III) Complexes of the Ligands: Samples of the Ln^{III} complexes for NMR measurements were prepared by dissolving $LnCl_3 \cdot 6H_2O$ and a 10% molar excess of the ligand in water, increasing the pH to about 7 with an aq. KOH solution and leaving the mixture for 1 h; ^{17}O-enriched water was added to the samples for ^{17}O variable-temperature and LIS NMR measurements to a concentration of about 0.5% ^{17}O. The samples for structural studies were prepared analogously, but in D_2O, to yield 0.1 M solutions of the complexes in all cases. The samples for ^{31}P NMR LIS were prepared in 20% D_2O. The pH of all resulting solutions was adjusted to 7 with either dilute HCl (DCl) or KOH (KOD). The absence of free Ln^{III} ions was verified by using xylenol orange as indicator in acetate buffer at a pH of about 5.5. Samples of the Eu^{III} complexes for UV/Vis spectroscopy were prepared analogously, and the samples originally prepared for NMR studies were used for luminescence experiments. The samples for measurements of ^1H NMRD profiles were prepared by exact dilution of the samples for ^{17}O NMR measurements to the final concentration of 5 mM.

X-ray Studies: Single crystals of all studied compounds were obtained by slow vapour diffusion of acetone into aqueous solutions of the compounds. For the complexes, dilute aq. LiOH was used for pH adjustment. The diffraction data were collected by using a Nonius Kappa CCD diffractometer (Enraf–Nonius) at 150(1) K with Mo-K_α radiation (λ = 0.71073 Å) and analysed by using the HKL program package.[55] The structures were solved by direct methods and refined by full-matrix least-squares techniques (SIR92[56] and SHELXL97[57]). Scattering factors for neutral atoms were included in the SHELXL97 program. Experimental data are given in Table 7. All non-hydrogen atoms in the structure of $H_4DOTP^{OEt} \cdot H_2O$ were refined anisotropically except for some disordered ethyl groups of the pendant arms. The hydrogen atoms belonging to the carbon atoms were fixed in the theoretical positions by using the riding model with $U_{eq}(H) = 1.2\,U_{eq}(C)$. Some hydrogen atoms attached to amino groups or oxygen atoms were located in the electron density difference map. In the case of the amino groups, the protons were fixed in the theoretical positions, and the protons of the oxygen atoms were refined in the original positions with thermal parameters $U_{eq}(H) = 1.2\,U_{eq}(X)$. All non-hydrogen atoms in the structure of $Li[Gd(DOTP^H)] \cdot 6H_2O$ were refined anisotropically, and all hydrogen atoms were fixed in their theoretical (C–H and P–H) or original (O–H) positions by using $U_{eq}(H) = 1.2\,U_{eq}(X)$. One pendant arm was best refined when turned into two positions (with *R* and *S* configuration on the phosphorus atom, respectively), and the lithium counterion was fitted in two positions as well (as it is coordinated by an oxygen atom of a partially occupied oxygen atom of a disordered phosphinate). All non-hydrogen atoms in the structure of $Li[Gd(DOTP^{OEt})] \cdot 0.5Me_2CO \cdot 8H_2O$ were refined anisotropically except for one disordered ethyl group of the pendant arms and one disordered water solvate molecule. The hydrogen atoms belonging to carbon atoms were fixed in their theoretical positions by using the riding model with $U_{eq}(H) = 1.2\,U_{eq}(C)$. Some of the hydrogen atoms attached to the solvate molecules were localized in the difference Fourier map and were treated in their original positions with $U_{eq}(H) = 1.2\,U_{eq}(O)$. CCDC-704357 ($H_4DOTP^{OEt} \cdot H_2O$), -704358 {$Li[Gd(DOTP^{OEt})] \cdot 0.5Me_2CO \cdot 8H_2O$}, and -704359 {$Li[Gd(DOTP^H)] \cdot 6H_2O$} contain the supplementary crystallographic data for this paper. These data can be obtained free of charge from The Cambridge Crystallographic Data Centre via www.ccdc.cam.ac.uk/data_request/cif.

Potentiometric Measurements: Potentiometric titrations were run, and the data obtained were treated according to a previously published procedure.[58] Protonation/dissociation and stability constants of H_4DOTP^H or H_4DOTP^{hm} and their complexes were determined in 0.1 M Me_4NCl at 25 °C. The stability constants of Gd^{III} complexes were obtained by the out-of-cell method with a waiting time for equilibrium of three weeks (some solutions were checked after six weeks and found to give the same data). Titrations were performed in the pH range 1.8–6.0 with around 30 data points per

Table 7. Crystallographic parameters of the studied compounds.

Compound	$H_4DOTP^{OEt} \cdot H_2O$	$Li[Gd(DOTP^H)] \cdot 6H_2O$	$Li[Gd(DOTP^{OEt})] \cdot 0.5Me_2CO \cdot 8H_2O$
Empirical formula	$C_{20}H_{50}N_4O_{13}P_4$	$C_{12}H_{40}GdLiN_4O_{14}P_4$	$C_{21.5}H_{63}GdLiN_4O_{20.5}P_4$
M_r	678.52	752.55	993.83
Colour,	colourless	colourless	colourless
Habit	rod	rod	prism
Crystal system	rhombic	monoclinic	rhombic
Space group	$Pca2_1$	$C2/c$	$P2_12_12_1$
a [Å]	19.4095(2)	17.5713(3)	14.2862(1)
b [Å]	13.4920(2)	6.9336(1)	24.2628(2)
c [Å]	24.5857(3)	22.3551(4)	25.0544(2)
β [°]	90	101.177(1)	90
V [Å^3]	6438.3(1)	2671.92(8)	8684.4(1)
Z	8	4	8
$D_{calcd.}$ [g cm^{-3}]	1.400	1.871	1.520
μ [mm^{-1}]	0.298	2.790	1.748
Total refl.	12198	3055	19853
Obsd. refl. [$I > 2\sigma(I)$]	10090	2965	17491
R	0.0535	0.0235	0.0395
R' [$I > 2\sigma(I)$]	0.0697	0.0246	0.0503
wR	0.1348	0.0581	0.0926
wR' [$I > 2\sigma(I)$]	0.1468	0.0589	0.0987

titration and three titrations per system. The pre-formed gadolinium(III) complexes in solution were obtained by mixing a known amount of ligand (5% molar excess) with $GdCl_3$ (as a defined stock solution) in a glass ampoule. A standard Me_4NOH solution (just to neutralize the ligand amount) was slowly added, and the ampoule was sealed and left at 80 °C overnight to fully complex the metal ion. The ampoules were opened, and aliquots of the solutions of the gadolinium(III) complexes were transferred to a titration vessel. Excess of HCl and Me_4NCl solutions were added (to reach a pH of about 2 and 0.1 M Me_4NCl in the final solution) and the solution was immediately titrated with a standard Me_4NOH solution up to a pH of about 12 at 25 °C, acquiring around 45 data points for each of three titrations.

EPR Measurements: X-band EPR spectra of aqueous solutions of the Gd^{III} chelates (1 mM, pH of about 7.0) were obtained at 25 °C by using a Bruker ESP-300E spectrometer operating at 9.43 GHz (0.34 T) with a quartz flat cell. Spectral acquisition parameters: sweep width: 40 mT; microwave power: 0.632 mW; modulation amplitude: 0.32 mT; time constant: 20.48 ms.

NMR and Relaxation Studies of the Lanthanide(III) Complexes: ^1H (300.0 MHz), ^{17}O (40.7 MHz) and ^{31}P (121.5 MHz) NMR spectra were acquired with a Varian VNMRS 300 spectrometer by using a 5 mm broadband probe. ^1H (400.0 MHz), ^{17}O (54.2 MHz) and ^{31}P (161.9 MHz) NMR spectra were also acquired with a Varian Unity INOVA 400 spectrometer and ^1H (500.0 MHz) and ^{31}P (202.3 MHz) NMR spectra with a Varian Unity 500 spectrometer using the same type of probe. BMS effects were corrected by using the internal D_2O lock signals. Water was used as solvent for the variable-temperature ^{17}O NMR shifts and LIS measurements, therefore no frequency lock could be applied. In this case, the correction for the BMS shifts was performed with the ^1H resonance of the internal standard *t*BuOH. H_3PO_4 (85%) was used as an external chemical shift reference for ^{31}P spectra. COSY spectra of some of the diamagnetic complexes were obtained by using 2048×2048 data points in F_1 and F_2. Pure absorption mode EXSY spectra were recorded by using the conventional NOESY 90°–t_1–90°–τ_{mix}–90°–acq. phase-sensitive pulse sequence in D_2O as solvent. The ^{31}P EXSY data were acquired with a variable mixing time between 2 and 150 ms and processed with the program Mestrec EXSY CALC v. 1.0.[59] Longitudinal relaxation rates ($1/T_1$) were obtained by the inversion-recovery method, and transverse relaxation rates ($1/T_2$) were measured by the Carr–Purcell–Meiboom–Gill spin-echo technique. At each temperature, the spectral parameters were measured for both the sample with gadolinium(III) complex and the sample of acidified water (pH 6) under exactly the same conditions. No frequency lock was applied. The $1/T_1$ nuclear magnetic relaxation dispersion (^1H NMRD) profiles of water protons at several temperatures (5, 25 and 37 °C) were obtained with a Stelar Master FFC-2000 relaxometer by using the field-cycling method and covering a continuum of magnetic fields from 2.35×10^{-4} to 0.35 T (corresponding to a proton Larmor frequency range from 0.01 MHz to 15 MHz). The spin-lattice proton relaxation rates at 0.47 (20) and 1.41 T (60 MHz) were measured with a Bruker Minispec mq-20 and a Bruker Minispec mq-60 spin analyzer, respectively. Relaxivity at different pH values (2–12) was measured with a Bruker Minispec mq-20 at 37 °C. The Ln^{III} contents in all samples were estimated from the bulk magnetic susceptibility (BMS) shift.[60]

Data Evaluation: Potentiometric data were evaluated with the program package OPIUM.[61] Relaxometric data were evaluated with Origin™, Version 6.0. All calculations using relaxometric data were carried out with least-squares fitting by the program SCIENTIST® for WINDOWS™ by Micromath® (ref.[62]) using a set of equations published previously.[27a] Molecular sizes of the complexes were estimated by constructing molecular models with HyperChem®, Version 7.5.[63]

Supporting Information (see footnote on the first page of this article): Molecular structures of two independent units found in the structure of $H_4DOTP^{OEt}\cdot H_2O$; UV/Vis spectra for the $^5D_0 \leftarrow {}^7F_0$ transition of $[Eu(DOTP^H)]^-$ and $[Eu(DOTP^{OEt})]^-$ complexes; $^{31}P\{^1H\}$ NMR spectra of Nd^{III}, Eu^{III} and Yb^{III} complexes of H_4DOTP^H, H_4DOTP^{hm}, H_4DOTP^{Et}, H_4DOTP^{OEt} and H_4DOTP^{OBu}; an example of a ^{31}P EXSY NMR spectrum for the $[Yb(DOTP^H)]^-$ complex; temperature dependence of the ^{31}P NMR spectra of the $[Yb(DOTP^{OEt})]^-$, $[Eu(DOTP^{OEt})]^-$ and $[Yb(DOTP^{hm})]^-$ complexes; ^1H NMR spectra of the $[Eu(DOTP^{hm})]^-$ and $[Eu(DOTP^{OEt})]^-$ complexes; schematic representation of the McConnel cone in the complexes; variable-temperature ^{17}O reduced relaxation rates and reduced angular frequencies of Gd^{III} complexes of H_4DOTP^H, H_4DOTP^{hm}, H_4DOTP^{OEt} and H_8DOTP; dependence of the relaxivity of the $[Gd(DOTP^{hm})]^-$ complex on pH; luminescence lifetimes (τ_{ex}) and the corresponding hydration numbers of selected Eu^{III} complexes.

Acknowledgments

We thank Prof. É. Tóth (CNRS, Orléans, France) for allowing us to measure UV/Vis spectra. This work was supported by the Grant Agency of the Czech Republic (grant no. 203/06/0467), the Czech Academy of Sciences (grant no. KAN201110651) and the Ministry of Education, Youth and Sport of the Czech Republic (grant no. MSM0021620857) and by the Foundation of Science and Technology (F.C.T.), Portugal (project PTDC/QUI/70063/2006 and grant SFRH/BD/9685/2002 to G. A. P.) and FEDER. This work was carried out in the framework of the COST D38 Action D38 "Metal-Based systems for Molecular Imaging Applications" and EU-FP6 "Network of Excellence" EMIL (grant no. LSHC-2004-503569) and DiMI (grant no. LSHB-2005-512146) projects.

[1] *The Chemistry of Contrast Agents in Medical Magnetic Resonance Imaging* (Eds.: A. E. Merbach, É. Tóth), Wiley, Chichester, England, **2001**.
[2] *Topics in Current Chemistry*, Springer Verlag, Heidelberg, **2002**, vol. 221.
[3] P. Caravan, J. J. Ellison, T. J. McMurry, R. B. Laufer, *Chem. Rev.* **1999**, *99*, 2293–2352.
[4] S. Aime, M. Botta, E. Terreno, *Adv. Inorg. Chem.* **2005**, *57*, 173–237.
[5] P. Hermann, J. Kotek, V. Kubíček, I. Lukeš, *Dalton Trans.* **2008**, 3027–3047.
[6] P. Caravan, *Chem. Soc. Rev.* **2006**, *35*, 512–523.
[7] A. Nonat, C. Gateau, P. H. Fries, M. Mazzanti, *Chem. Eur. J.* **2006**, *12*, 7133–7150.
[8] A. Borel, J. F. Bean, R. B. Clarkson, L. Helm, L. Moriggi, A. D. Sherry, M. Woods, *Chem. Eur. J.* **2008**, *14*, 2658–2667.
[9] M. Botta, *Eur. J. Inorg. Chem.* **2000**, 399–407.
[10] F. Avecilla, J. A. Peters, C. F. G. C. Geraldes, *Eur. J. Inorg. Chem.* **2003**, 4179–4186.
[11] S. Aime, M. Botta, E. Terreno, P. L. Anelli, F. Uggeri, *Magn. Reson. Med.* **1993**, *30*, 583–591.
[12] P. Caravan, M. T. Greenfield, X. Li, A. D. Sherry, *Inorg. Chem.* **2001**, *40*, 6580–6587.
[13] C. F. G. C. Geraldes, A. D. Sherry, I. Lázár, A. Miseta, P. Bogner, E. Berenyi, B. Sumegi, G. E. Kiefer, K. McMillan, F. Maton, R. N. Muller, *Magn. Reson. Med.* **1993**, *30*, 696–703.
[14] M. Murru, D. Parker, G. Williams, A. Beeby, *J. Chem. Soc., Chem. Commun.* **1993**, 1116–1118.

[15] J. Rohovec, P. Vojtíšek, P. Hermann, J. Mosinger, Z. Žák, I. Lukeš, *J. Chem. Soc., Dalton Trans.* **1999**, 3585–3592.

[16] a) S. Aime, A. S. Batsanov, M. Bota, J. A. K. Howard, D. Parker, K. Senanayake, G. Williams, *Inorg. Chem.* **1994**, *33*, 4696–4706; b) S. Aime, A. S. Batsanov, M. Botta, R. S. Dickins, S. Faulkner, C. E. Foster, A. Harrison, J. A. K. Howard, J. M. Moloney, T. J. Norman, D. Parker, L. Royle, J. A. G. Williams, *J. Chem. Soc., Dalton Trans.* **1997**, 3623–3636; R. L. Luck, C. L. Maupin, D. Parker, J. P. Riehl, J. A. G. Williams, *Inorg. Chim. Acta* **2001**, *317*, 331–337.

[17] S. Aime, M. Botta, M. Fasano, M. P. M. Marques, C. F. G. C. Geraldes, D. Pubanz, A. E. Merbach, *Inorg. Chem.* **1997**, *36*, 2059–2068.

[18] R. L. Luck, C. L. Maupin, D. Parker, J. P. Riehl, J. A. G. Williams, *Inorg. Chim. Acta* **2001**, *317*, 331–337.

[19] C. F. G. C. Geraldes, A. D. Sherry, G. E. Keifer, *J. Magn. Reson.* **1992**, *97*, 290–304.

[20] J. Rudovský, P. Cígler, J. Kotek, P. Hermann, P. Vojtíšek, I. Lukeš, J. A. Peters, L. Vander Elst, R. N. Muller, *Chem. Eur. J.* **2005**, *11*, 2373–2384.

[21] a) J. Rudovský, J. Kotek, P. Hermann, I. Lukeš, V. Mainero, S. Aime, *Org. Biomol. Chem.* **2005**, *3*, 112–117; b) J. Rudovský, M. Botta, P. Hermann, A. Koridze, S. Aime, *Dalton Trans.* **2006**, 2323–2333.

[22] P. Lebdušková, P. Hermann, L. Helm, É. Tóth, J. Kotek, K. Binnemans, J. Rudovský, I. Lukeš, A. E. Merbach, *Dalton Trans.* **2007**, 493–501.

[23] P. Vojtíšek, P. Cígler, J. Kotek, J. Rudovský, P. Hermann, I. Lukeš, *Inorg. Chem.* **2005**, *44*, 5591–5599.

[24] J. Kotek, J. Rudovský, P. Hermann, I. Lukeš, *Inorg. Chem.* **2006**, *45*, 3097–3102.

[25] a) S. Aime, E. Gianolio, D. Corpillo, C. Cavallotti, G. Palmisano, M. Sisti, G. B. Giovenzana, R. Pagliarin, *Helv. Chim. Acta* **2003**, *86*, 615–631; b) S. Aime, M. Botta, L. Frullano, S. Geninatti Crich, G. Giovenzana, R. Pagliarin, G. Palmisano, F. R. Sirtori, M. Sisti, *J. Med. Chem.* **2000**, *43*, 4017–4024; c) S. Aime, M. Botta, S. Geninatti Crich, G. Giovenzana, R. Pagliarin, M. Sisti, E. Terreno, *Magn. Reson. Chem.* **1998**, *36*, S200–S208.

[26] a) J. Kotek, P. Lebdušková, P. Hermann, L. Vander Elst, R. N. Muller, T. Maschmeyer, I. Lukeš, J. A. Peters, *Chem. Eur. J.* **2003**, *9*, 5899–5915; b) S. Aime, Z. Baranyai, E. Gianolio, K. Ramalingam, R. Swenson, R. Ranganathan, E. Brücher, S. Aime, *Contrast Media Mol. Imaging* **2007**, *2*, 94–102.

[27] a) P. Lebdušková, J. Kotek, P. Hermann, L. Vander Elst, R. N. Muller, I. Lukeš, J. A. Peters, *Bioconjugate Chem.* **2004**, *15*, 881–889; b) P. Lebdušková, A. Sour, L. Helm, É. Tóth, J. Kotek, I. Lukeš, A. E. Merbach, *Dalton Trans.* **2006**, 3399–3406.

[28] a) J. Rudovský, M. Botta, P. Hermann, K. I. Hardcastle, I. Lukeš, S. Aime, *Bioconjugate Chem.* **2006**, *17*, 975–987; b) J. Rudovský, P. Hermann, M. Botta, S. Aime, I. Lukeš, *Chem. Commun.* **2005**, 2390–2392.

[29] A. Borel, L. Helm, A. E. Merbach, *Chem. Eur. J.* **2001**, *7*, 600–610.

[30] a) E. Balogh, M. Mato-Iglesias, C. Platas-Iglesias, E. Tóth, K. Djanashvili, J. A. Peters, A. de Blas, T. Rodríguez-Blas, *Inorg. Chem.* **2006**, *45*, 8719–8728; b) M. Mato-Iglesias, E. Balogh, C. Platas-Iglesias, É. Tóth, A. de Blas, T. Rodríguez-Blas, *Dalton Trans.* **2006**, 5404–5415.

[31] K. Bazakas, I. Lukeš, *J. Chem. Soc., Dalton Trans.* **1995**, 1133–1137.

[32] M. Försterová, Z. Jandurová, F. Marques, L. Gano, P. Lubal, J. Vaněk, P. Hermann, I. Santos, *J. Inorg. Biochem.* **2008**, *102*, 1531–1540.

[33] L. Burai, R. Király, I. Lázár, E. Brücher, *Eur. J. Inorg. Chem.* **2001**, 813–820.

[34] M. Meyer, V. Dahaoui-Ginderey, C. Lecomte, R. Guilard, *Coord. Chem. Rev.* **1998**, *178–180*, 1313–1405.

[35] I. Lázár, D. C. Hrncir, W.-D. Kim, C. E. Kiefer, A. D. Sherry, *Inorg. Chem.* **1992**, *31*, 4422–4424.

[36] S. Aime, A. Barge, J. I. Bruce, M. Botta, J. A. K. Howard, J. M. Moloney, D. Parker, A. S. de Sousa, M. Woods, *J. Am. Chem. Soc.* **1999**, *121*, 5762–5771.

[37] I. Lukeš, J. Kotek, P. Vojtíšek, P. Hermann, *Coord. Chem. Rev.* **2001**, *216–217*, 287–312.

[38] J. Rohovec, M. Kývala, P. Vojtíšek, P. Hermann, I. Lukeš, *Eur. J. Inorg. Chem.* **2000**, 195–203.

[39] W. D. Kim, G. E. Kiefer, J. Huskens, A. D. Sherry, *Inorg. Chem.* **1997**, *36*, 4128–4134.

[40] J. Rohovec, I. Lukeš, P. Vojtíšek, I. Císařová, P. Hermann, *J. Chem. Soc., Dalton Trans.* **1996**, 2685–2691.

[41] I. Lázár, A. D. Sherry, R. Ramasamy, E. Brücher, R. Király, *Inorg. Chem.* **1991**, *30*, 5016–5019.

[42] R. Delgado, J. Costa, K. P. Guerra, L. M. P. Lima, *Pure Appl. Chem.* **2005**, *77*, 569–579.

[43] G. Anderegg, F. Arnaud-Neu, R. Delgado, J. Felcman, K. Popov, *Pure Appl. Chem.* **2005**, *77*, 1445–1495.

[44] A. D. Sherry, J. Ren, J. Huskens, E. Brücher, É. Tóth, C. F. G. C. Geraldes, M. M. Castro, W. P. Cacheris, *Inorg. Chem.* **1996**, *35*, 4604–4612.

[45] A. Bianchi, L. Calabi, C. Giorgi, P. Losi, M. Palma, P. Paoli, P. Rossi, B. Valtancoli, M. Virtuani, *J. Chem. Soc., Dalton Trans.* **2000**, 697–705.

[46] a) S. Aime, M. Botta, M. Fasano, E. Terreno, *Acc. Chem. Res.* **1999**, *32*, 941–949; b) S. Aime, E. Gianolio, A. Barge, D. Kostakis, I. C. Plakatouras, N. Hadjiljadis, *Eur. J. Inorg. Chem.* **2003**, 2045–2048; c) F. K. Kálmán, M. Woods, P. Caravan, P. Jurek, M. Spiller, G. Tircsó, R. Király, E. Brücher, A. D. Sherry, *Inorg. Chem.* **2007**, *46*, 5260–5270.

[47] W. W. De Horrocks Jr, D. R. Sudnick, *J. Am. Chem. Soc.* **1979**, *101*, 334–340.

[48] A. Beeby, I. M. Clarkson, R. S. Dickins, S. Faulkner, D. Parker, L. Royle, A. S. de Sousa, J. A. G. Williams, M. Woods, *J. Chem. Soc. Perkin Trans. 2* **1999**, 493–503.

[49] a) N. Graeppi, D. H. Powell, G. Laurenczy, L. Zékány, A. E. Merbach, *Inorg. Chim. Acta* **1995**, *235*, 311–326; b) É. Tóth, O. M. Ni Dhubhghaill, G. Besson, L. Helm, A. E. Merbach, *Magn. Reson. Chem.* **1999**, *37*, 701–708; c) F. Yerly, F. A. Dunand, É. Tóth, A. Figueirinha, Z. Kovács, A. D. Sherry, C. F. G. C. Geraldes, A. E. Merbach, *Eur. J. Inorg. Chem.* **2000**, 1001–1006; d) F. A. Dunand, S. Aime, S. G. Crich, G. B. Giovenzana, A. E. Merbach, *Magn. Reson. Chem.* **2002**, *40*, 87–92; e) M. Mato-Iglesias, C. Platas-Iglesias, K. Djanashvili, J. A. Peters, É. Tóth, E. Balogh, R. N. Muller, L. Vander Elst, A. de Blas, T. Rodríguez-Blas, *Chem. Commun.* **2005**, 4729–4731.

[50] a) S. Aime, M. Botta, D. Parker, J. A. G. Williams, *J. Chem. Soc., Dalton Trans.* **1995**, 2259–2266; b) S. Aime, M. Botta, R. C. Dickins, C. L. Maupin, D. Parker, J. P. Riehl, J. A. G. Williams, *J. Chem. Soc., Dalton Trans.* **1998**, 881–892.

[51] a) J. A. Peters, J. Huskens, D. J. Raber, *Prog. NMR Spectrosc.* **1996**, *28*, 283–350; b) K. Djanashvili, J. A. Peters, *Contrast Media Mol. Imaging* **2007**, *2*, 67–71.

[52] E. Zitha-Bovens, R. N. Muller, S. Laurent, L. Vander Elst, C. F. G. C. Geraldes, H. van Bekkum, J. A. Peters, *Helv. Chim. Acta* **2005**, *88*, 618–632.

[53] L. Vander Elst, A. Sessoye, S. Laurent, R. N. Muller, *Helv. Chim. Acta* **2005**, *88*, 574–587.

[54] D. H. Powell, O. M. N. Dhubhghaill, D. Pubanz, L. Helm, Y. S. Lebedev, W. Schlaepfer, A. E. Merbach, *J. Am. Chem. Soc.* **1996**, *118*, 9333–9346.

[55] Z. Otwinowski, W. Minor, *HKL Denzo and Scalepack Program Package by Nonius BV*, Delft, **1997**; Z. Otwinowski, W. Minor, *Methods Enzymol.* **1997**, *276*, 307–326.

[56] *SIR92, Program for Automatic Solution of Crystal Structures by Direct Methods*: A. Altomare, G. Cascarano, C. Giacovazzo, A. Guagliardi, M. C. Burla, G. Polidori, M. Camalli, *J. Appl. Crystallogr.* **1994**, *27*, 435–435.

[57] G. M. Sheldrick, *SHELXL97, Program for Crystal Structure Refinement from Diffraction Data*, University of Göttingen, Göttingen **1997**.

[58] a) P. Táborský, P. Lubal, J. Havel, J. Kotek, P. Hermann, I. Lukeš, *Collect. Czech. Chem. Commun.* **2005**, *70*, 1909–1942; b) M. Försterová, I. Svobodová, P. Lubal, P. Táborský, J. Kotek, P. Hermann, I. Lukeš, *Dalton Trans.* **2007**, 535–549.
[59] J. C. Cobas, M. Martín-Pastor, Universidade de Santiago de Compostella, **2004**.
[60] D. M. Corsi, C. Platas-Iglesias, H. van Bekkum, J. A. Peters, *Magn. Reson. Chem.* **2001**, *39*, 723–726.
[61] M. Kývala, I. Lukeš, *Chemometrics '95*, Abstract book, Pardubice, Czech Republic, **1995**, p. 63; full version of OPIUM program package is available (free of charge) on http://www.natur.cuni.cz/~kyvala/opium.html.
[62] *Scientist for Windows version 2.01*, Micromath Inc., Salt Lake City, UT, **1995**.
[63] *HyperChem. Release 7.5 for Windows*, Molecular Modeling System, Hypercube Inc., Ontario, Canada, **2002**.

Received: August 25, 2008
Published Online: November 7, 2008

